

Correlated Dephasing Noise in Single-photon Scattering

Tomás Ramos^{1,2} and Juan José García-Ripoll¹

¹ Instituto de Física Fundamental IFF-CSIC, Calle Serrano 113b, Madrid 28006, Spain

² Centro de Óptica e Información Cuántica, Facultad de Ciencias, Universidad Mayor, Chile

E-mail: t.ramos.delrio@gmail.com

30 October 2018

Abstract. We develop a theoretical framework to describe the scattering of photons against a two-level quantum emitter with arbitrary correlated dephasing noise. This is particularly relevant to waveguide-QED setups with solid-state emitters, such as superconducting qubits or quantum dots, which couple to complex dephasing environments in addition to the propagating photons along the waveguide. Combining input-output theory and stochastic methods, we predict the effect of correlated dephasing in single-photon transmission experiments with weak coherent inputs. We discuss homodyne detection and photon counting of the scattered photons and show that both measurements give the modulus and phase of the single-photon transmittance despite the presence of noise and dissipation. In addition, we demonstrate that these spectroscopic measurements contain the same information as standard time-resolved Ramsey interferometry, and thus they can be used to fully characterize the noise correlations without direct access to the emitter. The method is exemplified with paradigmatic correlated dephasing models such as colored Gaussian noise, white noise, telegraph noise, and $1/f$ -noise, as typically encountered in solid-state environments.

1. Introduction

The field of waveguide-QED [1,2] describes a variety of experimental setups where a quantum emitter interacts preferentially with a family of guided photonic modes, so that the emission rates γ_{\pm} into the waveguide approaches or even surpasses decay γ_{loss} into unwanted modes (see Figure 1). This regime has been achieved, for instance, in experiments with superconducting circuits [3–6], neutral atoms [7–10], molecules [11], and quantum dots in photonic crystals [12–14]. With a few exceptions, such as [15, 16], most experiments work in the Rotating-Wave Approximation (RWA) regime, allowing for an adequate description in terms of one- and few-photon wavefunctions [17–19], input-output theory [20–22], diagrammatic methods [23–25], and path integral formalism [26, 27]. Those descriptions usually do not account for other sources of error, such as dephasing, but we know that $1/f$ -noise severely affects all solid state devices [28], including quantum dots and superconducting circuits. There have been some experimental attempts at characterizing noise sources *outside* actual circuits, directly exploring the dynamics of the quantum scatterer using time-resolved methods [29–40] or Fourier transform spectroscopy [41–46]. Those detailed studies require time-resolved

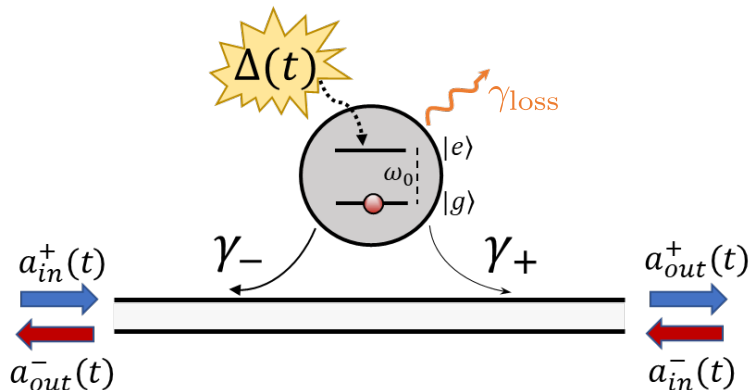


Figure 1. A noisy qubit with arbitrary correlated dephasing noise $\Delta(t)$ couples with rates γ_{\pm} to right- and left-propagating photons along a 1D waveguide. The qubit also decays with rate γ_{loss} into unguided modes. We model dephasing as a stochastic process, and photon scattering via input-output theory with operators $a_{in}^{\pm}(t)$ and $a_{out}^{\pm}(t)$.

measurements and direct control of the quantum scatterer in many cases, something which may be unfeasible or undesirable in waveguide-QED setups.

The purpose of this work is to develop a framework of waveguide-QED and scattering theory that accounts for general correlated dephasing, teaching us how to probe a qubit's noise and environment using few-photon scattering experiments. There are earlier works connecting noise with spectroscopy: Kubo's fluctuation-dissipation relations links dephasing to lineshapes in nuclear magnetic resonance (NMR) [47], as do later works in the field of quantum chemistry [48]. Our study complements those works, focusing on the quantum mechanical processes associated to single- and multiphoton scattering in waveguide-QED. We write down a stochastic version of the input-output formalism that consistently includes dephasing noise in the energy levels of the quantum emitter in addition to the dissipative dynamics due to the coupling to photons in the waveguide. We then relate the correlations in that noise to the average scattering matrix of individual photons and coherent wavepackets, and develop strategies to extract those correlations from actual experiments, in conjunction with earlier approaches to scattering tomography [49].

The paper and our main results are organized as follows. In Sec. 2 we introduce the model for a noisy two-level emitter in a waveguide. We describe dephasing noise as a stationary stochastic process $\Delta(t)$ and derive the stochastic input-output equations. In Sec. 3, we review the standard procedure of Ramsey interferometry and show how to quantify the noise correlations via the *Ramsey envelope* $C_{\phi}(t)$. We also introduce paradigmatic correlated noise models, which will be essential to understand the scattering results in the next sections. In particular, section 4 shows that the same information provided by Ramsey spectroscopy can be obtained from single-photon scattering experiments, where we only manipulate the qubit through the scattered photons. We solve the stochastic input-output equations for a qubit that interacts with a single propagating photon, and show that the *averaged single-photon scattering matrix* can be related one-to-one to the Ramsey envelope. We also discuss

analytical predictions for scattering under realistic dephasing models such as *colored Gaussian noise* and *1/f noise*. We show how the noise correlations modify the spectral lineshapes on each case, recovering simple limits such as the Lorentzian profiles that are fitted in most waveguide-QED experiments. Section 5 generalizes these ideas, showing how to measure the averaged scattering matrix using weak coherent state inputs together with homodyne or photon counting measurements, and how to reconstruct the Ramsey envelope $C_\phi(t)$ from such spectroscopic measurements. This opens the door to the reconstruction of more general correlated noise models that are non-Gaussian but common in many solid-state environments such as telegraph noise and 1/f noise due to ensembles of two-level fluctuators. We treat this separately in Appendix A due to the higher complexity of the stochastic methods needed for the analysis. We close this work in Sec. 6, discussing the conclusions and open questions.

2. Model for a noisy qubit in a photonic waveguide

Our study considers the setup depicted in Figure 1: a two-level quantum emitter or *qubit* is strongly coupled to a 1D photonic waveguide, emitting photons with rates γ_\pm along opposite directions, while simultaneously interacting with an unwanted environment that induces correlated dephasing and dissipation into unguided modes. The Hamiltonian of the total system can be decomposed as

$$H(t) = H_{\text{qb}}(t) + H_{\text{ph}} + H_{\text{qb-ph}}, \quad (1)$$

and below we describe each term.

First, the qubit Hamiltonian is given by

$$H_{\text{qb}}(t) = \frac{1}{2}[\omega_0 + \Delta(t)]\sigma_z, \quad (2)$$

where $\sigma_z = |e\rangle\langle e| - |g\rangle\langle g|$ is the diagonal Pauli operator, with $|e\rangle$ and $|g\rangle$ the excited and ground states of the qubit. We phenomenologically model environment-induced dephasing as a stochastic fluctuation $\Delta(t)$ of the qubit frequency around a mean value ω_0 . We assume the stochastic process $\Delta(t)$ [50–52] has vanishing mean —i.e. the *stochastic average* $\langle\langle \dots \rangle\rangle$ over noise realizations is zero $\langle\langle \Delta(t) \rangle\rangle = 0$ —, and is *stationary* —i.e. all expectation values and noise correlations $\langle\langle \Delta(t_1) \dots \Delta(t_n) \rangle\rangle$ are invariant under a global shift in time—. The simplest autocorrelation function $\langle\langle \Delta(0)\Delta(\tau) \rangle\rangle$ defines a characteristic correlation time τ_c of the noise as,

$$\tau_c = \int_0^\infty d\tau \frac{\langle\langle \Delta(0)\Delta(\tau) \rangle\rangle}{\langle\langle \Delta^2(0) \rangle\rangle}. \quad (3)$$

Those conditions and the machinery of stochastic methods [50–52] account for any realistic source of qubit dephasing, including arbitrary correlated Markovian and non-Markovian noise, or 1/f noise, among the examples considered below.

The second term in Eq. (1) corresponds to the Hamiltonian of free photons propagating in the waveguide and in unguided modes,

$$H_{\text{ph}} = \sum_{\mu=\pm} \int d\omega \omega a_\omega^\mu \dagger a_\omega^\mu + \int d\omega \omega b_\omega^\dagger b_\omega. \quad (4)$$

Here, the annihilation operator a_ω^μ destroys a photon of frequency ω propagating to the right ($\mu = +$) and left ($\mu = -$) of the waveguide, whereas b_ω destroys an unguided photon of frequency ω . They satisfy standard commutation relations $[a_\omega^\mu, a_{\omega'}^{\mu'\dagger}] = \delta_{\mu\mu'}\delta(\omega - \omega')$ and $[b_\omega, b_{\omega'}^\dagger] = \delta(\omega - \omega')$. We consider the RWA throughout this work, so that photons are only populated in a narrow bandwidth around the mean frequency of the qubit ω_0 , and the integration limits of ω in Eq. (4) can be safely extended to $\pm\infty$ [20, 54].

The last term in the Hamiltonian (1) describes the qubit-photon interaction, which in the RWA reads

$$H_{\text{qb-ph}} = \sum_{\mu=\pm} \sqrt{\frac{\gamma_\mu}{2\pi}} \int d\omega (\sigma^+ a_\omega^\mu + \text{h.c.}) + \sqrt{\frac{\gamma_{\text{loss}}}{2\pi}} \int d\omega (\sigma^+ b_\omega + \text{h.c.}), \quad (5)$$

with $\sigma^+ = |e\rangle\langle g|$ and $\sigma^- = |g\rangle\langle e|$ the raising and lowering qubit operators. The qubit absorbs and emits photons at a rate γ_μ for waveguide photons in direction $\mu = \pm$, and at a rate γ_{loss} for unguided photons. Assuming a Markov approximation in the qubit-photon coupling ($\gamma_\mu, \gamma_{\text{loss}}, |\Delta(t)| \ll \omega_0$), the dynamics of the photons can be integrated out, and the noisy qubit is effectively governed by quantum Langevin equations [20, 53, 54], given in the Heisenberg picture as

$$\frac{d\sigma^-}{dt} = - \left(\frac{\Gamma}{2} + i[\omega_0 + \Delta(t)] \right) \sigma^- + i\sigma_z \sum_{\mu=\pm} \sqrt{\gamma_\mu} a_{\text{in}}^\mu(t) + i\sigma_z \sqrt{\gamma_{\text{loss}}} b_{\text{in}}(t), \quad (6)$$

$$\frac{d\sigma_z}{dt} = - \Gamma(\sigma_z + 1) - 2i \sum_{\mu=\pm} \sqrt{\gamma_\mu} (\sigma^+ a_{\text{in}}^\mu(t) - \text{h.c.}) - 2i \sqrt{\gamma_{\text{loss}}} (\sigma^+ b_{\text{in}}(t) - \text{h.c.}). \quad (7)$$

Here, the total decay of the qubit $\Gamma = \gamma + \gamma_{\text{loss}}$, combines the emission of the qubit into guided $\gamma = \gamma_+ + \gamma_-$ and unguided modes γ_{loss} . While typical qubit-waveguide couplings are symmetric $\gamma_\pm = \gamma/2$, our formalism with independent channels ($\mu = \pm$) naturally admits the possibility of a ‘chiral’ waveguide with different couplings to left- and right-moving photons $\gamma_- \neq \gamma_+$ [55–57]. The initial condition of the photons is determined via the Heisenberg operators $a_{\text{in}}^\mu(t)$ and $b_{\text{in}}(t)$, which describe the input field photons in the waveguide and unguided modes, respectively, and read

$$a_{\text{in}}^\mu(t) = \frac{1}{\sqrt{2\pi}} \int d\omega e^{-i\omega(t-t_0)} a_\omega^\mu(t_0), \quad \text{and} \quad b_{\text{in}}(t) = \frac{1}{\sqrt{2\pi}} \int d\omega e^{-i\omega(t-t_0)} b_\omega(t_0), \quad (8)$$

with $a_\omega^\mu(t_0)$ and $b_\omega(t_0)$ the Heisenberg operators at the initial time.

After interacting with the qubit, the photons leave the waveguide through the right ($\mu = +$) and left ($\mu = -$) output ports, where they can be measured. The output fields of the waveguide photons are described by the output operators $a_{\text{out}}^\mu(t)$, which are given by input-output relations as [20, 53]

$$a_{\text{out}}^\mu(t) = a_{\text{in}}^\mu(t) - i\sqrt{\gamma_\mu} \sigma^-(t), \quad \text{with } \mu = \pm. \quad (9)$$

These equations allow us to access the information of the qubit’s dynamics via the waveguide photons and will be essential for the optical characterization of the correlated dephasing noise.

Due to the random classical field $\Delta(t)$, the equations of motion (6) and (7) are *stochastic* differential equations. In such equations, each particular realization of the noise provides

different quantum expectation values $\langle\sigma^{-}\rangle$ or $\langle\sigma_z\rangle$, and we need to average over all possible noise realizations to obtain more meaningful and measurable values —i.e. $\langle\langle\sigma^{-}\rangle\rangle$ or $\langle\langle\sigma_z\rangle\rangle$, as well as higher order multi-time correlations if needed—. In the remainder of the paper we calculate this kind of stochastic averages to characterize the effect of correlated dephasing noise on both the time-resolved dynamics (Sec. 3) and the single-photon spectroscopy (Secs. 4–5) of the qubit.

3. Time-resolved characterization of correlated dephasing noise

In this section, we first review the concepts of Ramsey interferometry (see Sec. 3.1) and then introduce the paradigmatic model of colored Gaussian noise (see Sec. 3.2), which can be analytically solved for arbitrary noise correlation times τ_c . Reviewing these concepts will be essential to understand the effect of correlated dephasing in the photon scattering of the next sections.

3.1. Ramsey interferometry

Ramsey interferometry [29, 30, 35] is the most common way to characterize qubit decoherence. This and other time-resolved methods require full control and read-out of the qubit, while it is in contact with its environment [see Figure 2(a)]. These methods are experimentally demanding, but give detailed information about noise correlations, specially when combined with dynamical decoupling [32, 37] and other control techniques [33, 36, 38, 39].

A standard Ramsey sequence consists of the five steps from figure 2(b): (i) Preparation of the qubit in its ground state $|g\rangle$, (ii) application of a Hadamard gate $H(0)$ with a very fast $\pi/2$ pulse, (iii) evolution of the qubit for a time t , (iv) application of a second Hadamard gate $H(t)$, and (v) measurement of the qubit population difference $\langle\sigma_z\rangle$. The purpose of steps (i)-(ii) is to produce the initial superposition state,

$$|\Psi(0)\rangle = H(0)|g\rangle|0\rangle = \frac{1}{\sqrt{2}}(|e\rangle + |g\rangle)|0\rangle, \quad (10)$$

for which the qubit coherence is maximal, namely $\langle\sigma^{-}(0)\rangle = 1/2$. Steps (iii)-(v) monitor the destruction of the qubit coherence $\langle\sigma^{-}(t)\rangle$, under the influence the noisy environment. Repeating this procedure for various waiting times t and averaging over many realizations, one obtains the average coherence $\langle\langle\sigma^{-}\rangle\rangle(t)$.

The dynamics of the qubit coherence under the influence of pure dephasing and radiative decay is obtained by taking expectation values on the quantum Langevin equation (6). For the initial condition (10), it reads

$$\frac{d}{dt}\langle\sigma^{-}\rangle = -\left(\frac{\Gamma}{2} + i[\omega_0 + \Delta(t)]\right)\langle\sigma^{-}\rangle, \quad (11)$$

which is a multiplicative stochastic differential equation with a random variable $\Delta(t)$ [50–52]. To solve for the average $\langle\langle\sigma^{-}\rangle\rangle(t)$, we integrate equation (11) formally and average the result

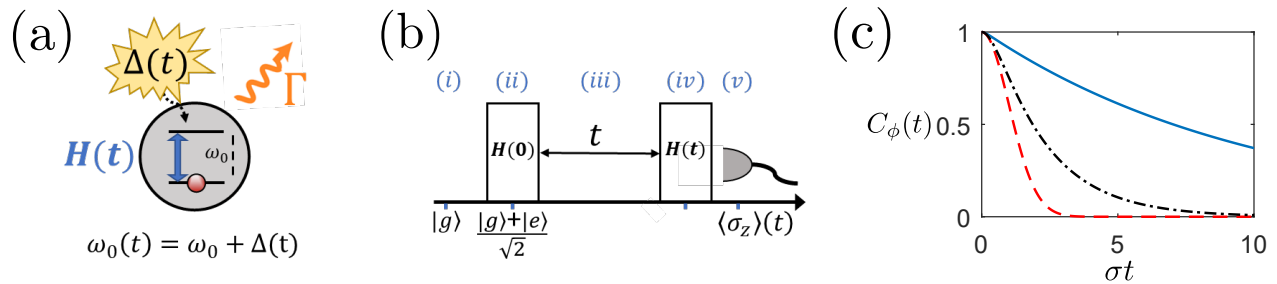


Figure 2. Time-resolved characterization of correlated dephasing noise. (a) A qubit coupled to a generic noisy environment causing pure dephasing $\Delta(t)$, and radiative relaxation with rate Γ . (b) Basic Ramsey sequence consisting of (i) ground state preparation, (ii) Hadamard gate $H(0)$, (iii) free evolution, (iv) second Hadamard gate $H(t)$, and (v) measurement of the qubit population difference $\langle\sigma_z\rangle(t)$. (c) Ramsey envelopes $C_\phi(t)$ for a noisy qubit with colored Gaussian dephasing, characterized by the noise strength σ and the correlation time $\tau_c = 1/\kappa$ (see Eq. (17)). For $\kappa = 10\sigma$ the noise is in the white limit and $C_\phi(t)$ is exponential (blue/solid line). For $\kappa = 0$ the noise is quasi-static and $C_\phi(t)$ is Gaussian (red/dashed line). Finally, for $\kappa = 2\sigma$ the decay interpolates between the two previous behaviors.

over all stochastic realizations of the random trajectory $\Delta(t)$, obtaining

$$\langle\langle\sigma^-\rangle\rangle = \frac{1}{2}e^{-(\Gamma/2+i\omega_0)t}C_\phi(t). \quad (12)$$

In addition to the exponential decay with rate Γ due to the coupling to photons \ddagger , pure dephasing originates an extra decay factor $C_\phi(t)$ known as Kubo’s relaxation function [47] or “Ramsey envelope” [33]. For stationary noise, $C_\phi(t)$ is the average of the random phase accumulated by the qubit after a time t , namely

$$C_\phi(t) = \langle\langle e^{-i\int_0^t dt' \Delta(t')} \rangle\rangle. \quad (14)$$

In general, this function depends on noise correlations of arbitrary order $\langle\langle\Delta(t_1)\dots\Delta(t_n)\rangle\rangle$ whose characterization requires sophisticated noise spectroscopy methods [38, 58], but for Gaussian noise we will find that only first and second moments are required, as shown below.

3.2. Colored Gaussian noise, white noise, and quasi-static noise

For stationary Gaussian noise with vanishing mean, all cumulants and correlations can be expressed in terms of the autocorrelation $\langle\langle\Delta(0)\Delta(\tau)\rangle\rangle$ [47, 51], and thus $C_\phi(t)$ in Eq. (14) is reduced to

$$C_\phi(t) = \exp\left(-\int_0^t d\tau(t-\tau)\langle\langle\Delta(0)\Delta(\tau)\rangle\rangle\right). \quad (15)$$

\ddagger Notice that the relaxation decay Γ can be obtained independently of the dephasing noise by measuring $\langle\langle\sigma_z\rangle\rangle$ without the second Hadamard gate in Figure 2, resulting in the pure exponential decay,

$$\langle\langle\sigma_z\rangle\rangle = e^{-\Gamma t} - 1. \quad (13)$$

If the noise is also Markovian, Doob's theorem [51] implies that the noise can be described as an Ornstein-Uhlenbeck process [50–52] with autocorrelation given explicitly by

$$\langle\langle\Delta(0)\Delta(\tau)\rangle\rangle = \sigma^2 e^{-\kappa|\tau|}. \quad (16)$$

This rich model describes “colored Gaussian noise” with strength $\sigma = \langle\langle\Delta^2(0)\rangle\rangle^{1/2}$ and a correlation time $\tau_c = 1/\kappa$, that covers both fast and slow noise limits. This includes *white noise* with autocorrelation $\langle\langle\Delta(0)\Delta(\tau)\rangle\rangle = 2\gamma_\phi\delta(\tau)$, when taking the limits $\kappa \rightarrow \infty$ and $\sigma \rightarrow \infty$, while keeping a constant pure dephasing rate $\gamma_\phi = \sigma^2/\kappa$. It also includes *quasi-static noise* in the opposite limit of $\kappa \rightarrow 0$, in which the autocorrelation becomes constant $\langle\langle\Delta(0)\Delta(\tau)\rangle\rangle = \sigma^2$.

Another advantage of the colored Gaussian noise (16) is that the Ramsey envelope (15) can be derived analytically

$$C_\phi(t) = \exp\left(-(\sigma/\kappa)^2(e^{-\kappa t} + \kappa t - 1)\right). \quad (17)$$

This super-exponential envelope has been fitted to experimental data to quantify the strength and correlation of realistic environments [29, 33]. Figure 2(c) shows the typical shape of this envelope in the limits of fast and slow noise. In the white noise limit (blue/solid line), the decay is exponential $C_\phi(t) = \exp(-\gamma_\phi t)$ with $\gamma_\phi = \sigma^2/\kappa$; in the quasi-static limit (red/dashed), the decay is Gaussian $C_\phi(t) = \exp(-\sigma^2 t^2/2)$; and for intermediate values such as $\kappa = 2\sigma$, the curve clearly interpolates between both shapes (black/dotted).

4. Single-photon scattering from a qubit with correlated dephasing noise

In the following we use the stochastic input-output formalism of Sec. 2 to compute the average single-photon scattering matrix for a qubit with stationary dephasing noise $\Delta(t)$. Most importantly, in Sec. 4.1 we derive the stochastic differential equation to solve for the average transmittance $\langle\langle t_\omega^\mu \rangle\rangle$ and reflectance $\langle\langle r_\omega^\mu \rangle\rangle$ in a single-photon scattering experiment. In the spirit of Kubo [47], we also show that these scattering coefficients contain the same noise correlations as the Ramsey envelope $C_\phi(t)$, which can be determined by an independent time-resolved experiment as shown in the previous section. Finally, we evaluate $\langle\langle t_\omega^\mu \rangle\rangle$ for a qubit with colored Gaussian noise (see Sec. 4.2) and 1/f noise (see Sec. 4.3), discussing on each case the broadening of the spectral lineshape and the connections to well known results in the literature.

4.1. Average single-photon scattering matrix

The *single-photon scattering matrix* $S_{\nu\omega}^{\lambda\mu}$ describes the interaction between an isolated photon and a quantum emitter. It is defined as the probability amplitude for the emitter to transform an incoming photon with frequency ω in channel $\mu = \pm$ into an outgoing photon with possibly different frequency ν and direction $\lambda = \pm$:

$$S_{\nu\omega}^{\lambda\mu} = \langle g | \langle 0 | a_{\text{out}}^\lambda(\nu) a_{\text{in}}^{\mu\dagger}(\omega) | g \rangle | 0 \rangle. \quad (18)$$

The monochromatic input-output photonic operators $a_{\text{in}}^\mu(\omega)$ and $a_{\text{out}}^\mu(\omega)$ are given by the Fourier transform \mathcal{F} of the Heisenberg input-output field amplitudes defined above [20]:

$$a_{\text{in}}^\mu(\omega) = \mathcal{F}[a_{\text{in}}^\mu(t)](\omega), \quad a_{\text{out}}^\mu(\omega) = \mathcal{F}[a_{\text{out}}^\mu(t)](\omega), \quad (19)$$

with $\mathcal{F}[f(t)](\omega) = (2\pi)^{-1/2} \int_{-\infty}^{\infty} dt e^{i\omega t} f(t)$ for a test function $f(t)$. Notice that these monochromatic operators (19) satisfy canonical bosonic commutation relations as well as their time-domain counterparts, namely $[a_{\text{in}}^\lambda(\nu), a_{\text{in}}^{\mu\dagger}(\omega)] = [a_{\text{out}}^\lambda(\nu), a_{\text{out}}^{\mu\dagger}(\omega)] = \delta_{\lambda\mu} \delta(\nu - \omega)$.

The scattering matrix of the noisy qubit is derived by combining equations (9), (18), and (19) to obtain

$$S_{\nu\omega}^{\lambda\mu} = \delta_{\lambda\mu} \delta(\nu - \omega) - \sqrt{\frac{\gamma_\lambda \gamma_\mu}{2\pi}} \mathcal{F}[G_\omega(t)](\nu - \omega). \quad (20)$$

Here, the *scattering overlap*, $G_\omega(t) = ie^{i\omega t} (2\pi/\gamma_\mu)^{1/2} \langle 0 | \sigma^-(t) a_{\text{in}}^{\mu\dagger}(\omega) | 0 \rangle$ satisfies an inhomogeneous stochastic differential equation derived from Eqs. (6)-(7),

$$\frac{dG_\omega}{dt} = - \left(\frac{\Gamma}{2} - i[\omega - \omega_0] + i\Delta(t) \right) G_\omega(t) + 1, \quad (21)$$

and with initial condition $G_\omega(t_0) = 0$ for $t_0 \rightarrow -\infty$. This is similar to the equation for the qubit's coherence (11), but now including a constant source term.

As explained in Sec. 5, spectroscopic measurements are not related to S but to the average scattering matrix $\langle\langle S_{\nu\omega}^{\lambda\mu} \rangle\rangle$. Computing this quantity is a two-step process. First, we formally integrate equation (21) for a stationary noise $\Delta(t)$ and solve for the average $\langle\langle G_\omega(t) \rangle\rangle$. Using the stationary noise property $\langle\langle e^{-i \int_{t-\tau}^t dt' \Delta(t')} \rangle\rangle = \langle\langle e^{-i \int_0^\tau dt' \Delta(t')} \rangle\rangle = C_\phi(\tau)$ and taking the limit $t_0 \rightarrow -\infty$, we find that the solution is independent of time, namely

$$\langle\langle G_\omega(t) \rangle\rangle = \langle\langle G_\omega \rangle\rangle = \mathcal{L}[C_\phi(\tau)](\Gamma/2 - i[\omega - \omega_0]). \quad (22)$$

Note how the noise correlations enter via the Kubo relaxation function $C_\phi(t)$ in Eq. (14) after a Laplace transform $\mathcal{L}[f(t)](s) = \int_0^\infty dt e^{-st} f(t)$. The second step is to take the stochastic average in Eq. (20) and insert the Fourier transform of Eq. (22) which is trivially given by $\mathcal{F}[\langle\langle G_\omega(t) \rangle\rangle](\nu - \omega) = \sqrt{2\pi} \langle\langle G_\omega \rangle\rangle \delta(\nu - \omega)$. The total averaged scattering matrix then reads

$$\langle\langle S_{\nu\omega}^{\lambda\mu} \rangle\rangle = \{ \delta_{\lambda\mu} - \sqrt{\gamma_\lambda \gamma_\mu} \langle\langle G_\omega \rangle\rangle \} \delta(\nu - \omega), \quad (23)$$

where the delta function $\delta(\nu - \omega)$ indicates that the scattering conserves the energy of the photons *on average*. On each realization, we can imagine the emitter absorbing a photon when its transition frequency is $\omega_0 + \Delta(t)$, and then relaxing by spontaneous emission when it has a different frequency $\omega_0 + \Delta(t')$. During this process, the dephasing environment exerts work on the qubit, adding and subtracting energy via the external field $\Delta(t)$, even though the total work is zero on average. The system of qubit and photons is thus an open system due to the presence of the dephasing environment and must be described by a mixed state in general. Nevertheless, this is not relevant when we focus on the scattered photons on the same frequency mode as the input. The averaged single-photon transmittance $\langle\langle t_\omega^\mu \rangle\rangle$ and reflectance $\langle\langle r_\omega^\mu \rangle\rangle$ are directly given by the pre-factors in Eq. (23) as

$$\langle\langle t_\omega^\mu \rangle\rangle = 1 - \gamma_\mu \mathcal{L}[C_\phi(t)](\Gamma/2 - i[\omega - \omega_0]), \quad (24)$$

$$\langle\langle r_\omega^\mu \rangle\rangle = -\sqrt{\gamma_+ \gamma_-} \langle\langle G_\omega \rangle\rangle = \sqrt{\gamma_- / \gamma_+} (\langle\langle t_\omega^\mu \rangle\rangle - 1), \quad (25)$$

and measure the average amplitude of the photons on the same ($\lambda = \mu$) and opposite ($\lambda = -\mu$) output channel. with respect to the input beam μ . Notice that the asymmetry in the couplings $\gamma_+ \neq \gamma_-$ appears in Eqs. (24)-(25) as a pre-factor of $\langle\langle G_\omega \rangle\rangle$ and thus it only rescales the lineshape of the qubit. For the scope of the present paper it is therefore enough to consider examples in the symmetric case only ($\gamma_\mu = \gamma/2$), but we will still keep all the formulas general.

Equations (21)-(25) have deep physical meaning as they allow us to predict the spectroscopic lineshape of a noisy qubit either by solving the stochastic differential equation (21) or by using the knowledge of the Ramsey envelope $C_\phi(t)$ obtained independently via standard time-resolved noise experiments. In Ref. [47], Kubo used the fluctuation-dissipation theorem to find a similar relation between $C_\phi(t)$ and the noise power spectrum, but this quantity is generic and not as simple to measure in a scattering experiment as the average transmittance we have introduced (see Sec. 5).

Finally, we would like to remark that the present derivation may be easily extended in various manners. So far we have considered a noisy qubit that is perfectly “side-coupled” to the waveguide, but in experiments there may be impedance mismatches and internal reflections that cause Fano resonance in the scattering profiles [59, 60]. Therefore, Appendix B generalizes Eqs. (24)-(25) for a noisy qubit with a Fano resonance and shows that the corresponding relations between transmission and reflection coefficients are still valid under correlated dephasing noise. On the other hand, it is also possible to include multiple noise sources on the qubit. In this respect, Appendix C shows that adding a white noise background $\Delta_{\text{WB}}(t)$ to correlated noise, i.e. $\Delta(t) \rightarrow \Delta(t) + \Delta_{\text{WB}}(t)$, amounts to a trivial replacement $\Gamma/2 \rightarrow \Gamma/2 + \gamma_{\text{WB}}$ in the stochastic equation (21), where γ_{WB} is the pure dephasing rate of the white noise background.

4.2. Average transmittance of qubit with colored Gaussian dephasing

In spectroscopy, correlated dephasing is typically referred to as *spectral diffusion* [42–45] because it broadens the lineshapes of emitters. In this subsection we analyze this broadening and the average single-photon transmittance $\langle\langle t_\omega^\mu \rangle\rangle$ of a qubit with colored Gaussian dephasing noise (see Sec. 3.2 for details on the model), paying special attention to the limits of white and quasi-static noise where the transmittance exhibits qualitatively different behaviors.

Equation (24) provides an expression for the single-photon transmittance $\langle\langle t_\omega^\mu \rangle\rangle$ in terms of the analytical Ramsey envelope in Eq. (17). For colored Gaussian noise with arbitrary correlation time $\tau_c = 1/\kappa$ and noise strength σ we can either estimate numerically the Laplace transform, or expand the super-exponential function in a power series to obtain

$$\langle\langle t_\omega^\mu \rangle\rangle = 1 - \gamma_\mu \sum_{n=0}^{\infty} \frac{(-1)^n}{n!} \frac{e^{(\sigma/\kappa)^2} (\sigma/\kappa)^{2n}}{\Gamma/2 + \sigma^2/\kappa + n\kappa - i(\omega - \omega_0)}. \quad (26)$$

In the limit of white noise ($\kappa, \sigma \rightarrow \infty$ with σ^2/κ fixed), only the term with $n = 0$ survives in

Eq. (26), and the average transmittance is a Lorentzian function§,

$$\langle\langle t_\omega^\mu \rangle\rangle = 1 - \frac{\gamma_\mu}{\Gamma/2 + \gamma_\phi - i(\omega - \omega_0)}, \quad (27)$$

with pure dephasing rate $\gamma_\phi = \sigma^2/\kappa$. This is a well-known result, typically proven via the master equation formalism [61], which demonstrates that white noise pure dephasing maintains the natural Lorentzian lineshape of the qubit, while its width and depth get modified by γ_ϕ [3, 11, 59]. This Lorentzian behavior is shown by the blue/solid transmittance in Figure 3(a), for typical waveguide QED parameters. If we now consider a finite but moderate correlation time $\sigma \lesssim \kappa < \infty$, more and more terms in the series expansion (26) become important, resulting in a transmittance with a larger width and smaller depth, as shown by the black/dash-dotted curve in Figure 3(a). Finally, in the quasi-static limit of very long correlation times $\kappa \ll \sigma < \infty$, all terms in Eq. (26) contribute and the series expansion fails to converge numerically. In this case, we make the approximation $\kappa \rightarrow 0$ in which the relaxation function (17) is Gaussian, $C_\phi(t) = \exp(-\sigma^2 t^2/2)$, and perform the required Laplace transform analytically, obtaining||

$$\langle\langle t_\omega^\mu \rangle\rangle = 1 - \frac{\gamma_\mu}{\sigma} \sqrt{\frac{\pi}{2}} e^{\frac{(\Gamma/2 - i[\omega - \omega_0])^2}{2\sigma^2}} \operatorname{erfc}\left(\frac{\Gamma/2 - i[\omega - \omega_0]}{\sqrt{2}\sigma}\right), \quad (28)$$

with the *complementary error function* $\operatorname{erfc}(z) = (2/\sqrt{\pi}) \int_z^\infty dx e^{-x^2}$. From equation (28) we conclude that in the slow noise limit $\kappa \ll \sigma < \infty$, $\langle\langle t_\omega^\mu \rangle\rangle$ is Gaussian-like and has a width proportional to the noise strength σ . This behavior is shown by the red/dashed transmittance from figure 3(a). Notice that the Lorentzian (blue/solid) and Gaussian-like (red/dashed) lineshape limits can be qualitatively distinguished in transmittance experiments by their width, curvature, and tails [62], suggesting that spectroscopy can be a simple approach to discover the noise correlation properties. More specifically, fitting arbitrary parameters κ and σ to experimental transmittance data $\langle\langle t_\omega^\mu \rangle\rangle$ one may even quantify the correlation time $\tau_c = 1/\kappa$ and the noise strength σ of a given environment as recently done in Ref. [5].

Colored Gaussian noise is a useful and powerful dephasing model, and thus it is tempting to assume that this is the real noise. Indeed, this is what is done in most common waveguide-QED experiments, where a Lorentzian profile is assumed and a single dephasing parameter γ_ϕ is fitted [3]. In Sec. 5 we will show that there is a more general approach, using estimates of the transmittance $\langle\langle t_\omega^\mu \rangle\rangle$ to extract the Ramsey profile and noise correlations, in a single-photon scattering protocol that generalizes current experiments [see Figure 3(b)].

4.3. Average transmittance of a qubit with $1/f$ dephasing noise

In this subsection, we consider a noisy qubit with dephasing due to $1/f$ noise, a very slowly varying, highly correlated, and low-frequency noise that is ubiquitously encountered

§ In the white noise limit, Eq. (17) becomes the exponential $C_\phi(t) = \exp(-\gamma_\phi t)$, so that the Lorentzian lineshape follows directly from the Laplace transform in Eq. (24).

|| This expression can also be obtained by a simple static average over noiseless Lorentzian transmittances with different qubit frequencies as $\langle\langle t_\omega^\mu \rangle\rangle = 1 - \gamma_\mu \int d\Delta P_G(\Delta)/(\Gamma/2 - i[\omega - \omega_0] + i\Delta)$, where $P_G(\Delta) = (2\pi\sigma^2)^{-1/2} e^{-\Delta^2/(2\sigma^2)}$ is a Gaussian probability distribution with standard deviation σ .

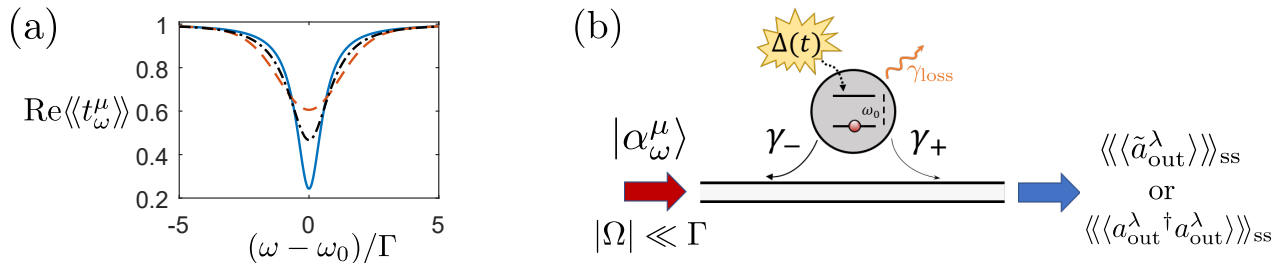


Figure 3. (a) Average single-photon transmittance $\langle\langle t_\omega^\mu \rangle\rangle$ of a noisy qubit coupled to a 1D photonic waveguide with parameters $\gamma_\pm = \gamma/2$, $\gamma = 0.9\Gamma$, and $\gamma_{\text{loss}} = 0.1\Gamma$. We consider a colored Gaussian dephasing model, characterized by the correlation time $\tau_c = 1/\kappa$ and the noise strength $\sigma = \Gamma$. For $\kappa = 10\sigma$, the noise is in the white limit and the transmittance has a Lorentzian lineshape (blue/solid). For $\kappa = 0$ the noise is quasi-static and $\langle\langle t_\omega^\mu \rangle\rangle$ is Gaussian-like as given in Eq. (28) (red/dashed). Finally, for $\kappa = 2\sigma$ the transmittance interpolates between two previous behaviors (black/dash-dotted). (b) Measurement of $\langle\langle t_\omega^\mu \rangle\rangle$ of a noisy qubit in a waveguide, using a coherent state input ($|\Omega| \ll \Gamma$), and homodyne or power measurements at the output.

in electronics and solid-state devices such as superconducting qubits or quantum dots [28]. Nowadays there is still ongoing research on the microscopic origin and universal mechanisms behind this type of noise [63–67], but an unquestionable experimental evidence is that its *noise power spectrum*, $\mathcal{S}(\omega) = \sqrt{2\pi}\mathcal{F}[\langle\langle\Delta(0)\Delta(\tau)\rangle\rangle](\omega)$, presents a power-law behavior $\mathcal{S}(\omega) \propto 1/\omega^\eta$, with $0 < \eta < 2$. In fact, it is exactly this low frequency divergence what makes 1/f noise so difficult to filter and to controllably observe in experiments [28].

There have been various proposals for phenomenologically modeling the effects of 1/f noise within a finite but broad frequency window $\kappa_{\min} \ll \omega \ll \kappa_{\max}$ [68–72]. The basic assumption is that it is produced by a sum of N uncorrelated noise sources,

$$\Delta(t) = \frac{1}{\sqrt{N}} \sum_{j=1}^N \Delta_j(t), \quad (29)$$

with noise components $\Delta_j(t)$ presenting correlations of the form $\langle\langle\Delta_j(0)\Delta_j(\tau)\rangle\rangle = \sigma_j^2 e^{-\kappa_j|\tau|}$, and thus the total autocorrelation and noise spectrum read

$$\langle\langle\Delta(0)\Delta(\tau)\rangle\rangle = \frac{1}{N} \sum_{j=1}^N \sigma_j^2 e^{-\kappa_j|\tau|}, \quad \text{and} \quad \mathcal{S}(\omega) = \frac{1}{N} \sum_{j=1}^N \frac{2\kappa_j\sigma_j^2}{\kappa_j^2 + \omega^2}. \quad (30)$$

To achieve this situation, the noise components $\Delta_j(t)$ can be modeled as independent Ornstein-Uhlenbeck processes [72] (Sec. 3.2), but it is also typically assumed that $\Delta_j(t)$ are originated by an ensemble of two-level fluctuators [68–70], characterized by different noise strengths σ_j and jumping rates κ_j (see Appendix A.2). In either case, if the parameters κ_j present an uniform distribution of $\log_{10}(\kappa_j/\Gamma)$ in a broad range from $\kappa_1 = \kappa_{\min}$ to $\kappa_N = \kappa_{\max}$, and if $\sigma_j = \sigma_1(\kappa_1/\kappa_j)^{(\eta-1)/2}$, then in the limit $N \gg 1$ the noise spectrum $\mathcal{S}(\omega)$ in Eq. (30) approximates a power-law behavior [72],

$$\mathcal{S}(\omega) \approx \left[\frac{\pi\sigma_1^2\kappa_1^{\eta-1}}{\sin(\pi\eta/2)\ln(\kappa_N/\kappa_1)} \right] \frac{1}{\omega^\eta}, \quad \text{for } \kappa_1 \ll \omega \ll \kappa_N. \quad (31)$$

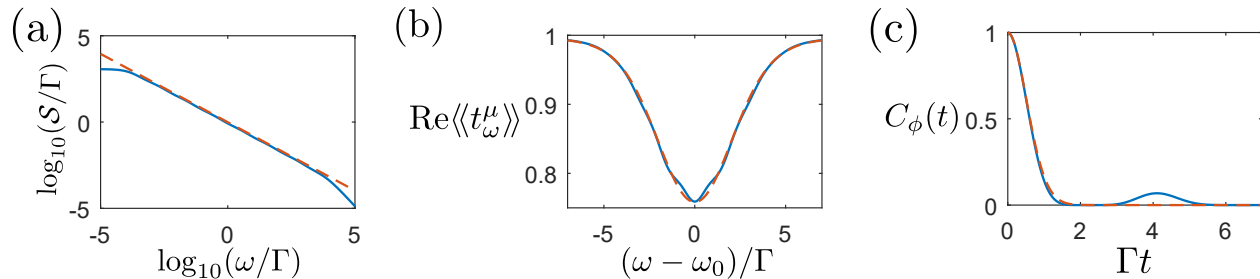


Figure 4. Noisy qubit with $1/f$ dephasing noise. (a) Noise power spectrum $S(\omega)$ for $1/f^{0.99}$ noise (red/dashed), and its simulation by $N = 8$ uncorrelated noises (blue/solid) with $\kappa_1 = 10^{-5}\Gamma$, $\kappa_N = 10\Gamma$, and $\sigma_1 = 2\Gamma$, as indicated in Eqs. (31) and (30), respectively. (b) Average transmittance $\langle\langle t_\omega^\mu \rangle\rangle$ for qubit with the $1/f^{0.99}$ dephasing noise model in (a), and the waveguide parameters $\gamma_\pm = \gamma/2$, $\gamma = 0.9\Gamma$, and $\gamma_{\text{loss}} = 0.1\Gamma$. The red/dashed curve corresponds to Gaussian $1/f^{0.99}$ noise and the blue/solid to non-Gaussian $1/f^{0.99}$ noise caused $N = 8$ different two-level fluctuators (see Appendix A). (c) Time-resolved Ramsey envelope $C_\phi(t)$ corresponding to the same parameters and same line-types as in (b).

In Figure 4(a) we illustrate the effectiveness of this method with a numerical simulation of $1/f^{0.99}$ noise with only $N = 8$ independent noise components. We see that that exact noise spectrum in Eq. (30) (blue/solid), approximates well the expected the power-law behavior (red/dashed) in the frequency range $10^{-4} \ll \omega/\Gamma \ll 10^4$.

Now we solve for the average transmittance $\langle\langle t_\omega^\mu \rangle\rangle$ and the Ramsey envelope $C_\phi(t)$ for a noisy qubit subject to the above model of $1/f$ noise. We can simulate Gaussian or non-Gaussian $1/f$ noise depending if we choose the noise components $\Delta_j(t)$ in Eq. (29) as colored Gaussian noises (see Sec. 4.2) or as an ensemble of two-level fluctuators (see Appendix A.4). In the former case, $C_\phi(t)$ in Eq. (15) can be analytically computed from the autocorrelation (30), and reads

$$C_\phi(t) = \exp\left(-\frac{1}{N} \sum_{j=1}^N (\sigma_j/\kappa_j)^2 (e^{-\kappa_j t} + \kappa_j t - 1)\right), \quad (32)$$

where κ_j and σ_j are chosen to simulate the $1/f$ model as explained above. To obtain $\langle\langle t_\omega^\mu \rangle\rangle$ we use Eq. (24) and numerically calculate the Laplace transform of Eq. (32) as done in Sec. 3.2 for a single colored Gaussian noise. On the other hand, calculating $\langle\langle t_\omega^\mu \rangle\rangle$ for non-Gaussian $1/f$ noise requires more advanced stochastic methods for describing the dynamics of the two-level fluctuators. This is done in full detail in Appendix A, but here we discuss the results. In Figures 4(b) and (c) we display $\langle\langle t_\omega^\mu \rangle\rangle$ and $C_\phi(t)$ for a noisy qubit with dephasing due to the $1/f^{0.99}$ noise simulated in Figure 4(a), and typical waveguide QED parameters. The red/dashed lines are the predictions in the Gaussian case as calculated via Eq. (32), whereas the blue/solid lines correspond to the non-Gaussian situation, calculated from Eqs. (A.20)-(A.22). The main difference between Gaussian and non-Gaussian $1/f$ noises are small bumps in $\langle\langle t_\omega^\mu \rangle\rangle$ and $C_\phi(t)$, which are signatures of the sparsity or granularity of the dephasing environment as treated in detail in Appendix A.3. Besides that, both predictions agree well and behave very similar to a single colored Gaussian noise in the quasi-static limit,

except for the power-law spectrum $\mathcal{S}(\omega)$.

5. Spectroscopic characterization of correlated dephasing noise

This section introduces a simple experimental protocol to measure the average single-photon transmittance and reflectance, and to recover the correlated dephasing noise from those quantities. This protocol only requires attenuated coherent states and either homodyne or power measurements at the output —the choice of which depends mainly on whether the experiment is performed with microwave [3, 5] or optical photons [60, 73, 74]—. In Sec. 5.1 we summarize and discuss the most important results to apply the protocol, while Sec. 5.2 contains details on the derivation. In addition to this, Appendix B generalizes the protocol to the case the noisy qubit sees Fano resonances [75, 76], as for instance, in experiments with quantum dots in photonic crystals waveguides [59, 60, 77].

5.1. Results of the protocol

The experimental procedure is sketched in Figure 3(b), where a monochromatic coherent state $|\alpha_\omega^\mu\rangle$ of amplitude α_ω^μ and frequency ω is injected on the input channel $\mu = \pm$ of the waveguide. We study the evolution of the corresponding initial state

$$|\Psi(0)\rangle = |\Psi_{\text{qb}}\rangle |\alpha_\omega^\mu\rangle, \quad (33)$$

which describes a coherently driven qubit from an arbitrary initial state $|\Psi_{\text{qb}}\rangle$, and vacuum states in all photonic channels different than μ . We will work in the limit of weak driving $|\Omega| \ll \Gamma$, with driving strength given by $\Omega = -i\alpha_\omega^\mu\sqrt{\gamma_\mu}$. We show below that in this limit we recover the single-photon transmittance from homodyne or power measurements in steady state, as follows

$$\frac{\langle\langle \tilde{a}_{\text{out}}^\mu \rangle\rangle_{\text{ss}}}{\alpha_\omega^\mu} = \langle\langle t_\omega^\mu \rangle\rangle + \mathcal{O}[|\Omega|/\Gamma]^2, \quad (34)$$

$$\frac{\langle\langle a_{\text{out}}^\mu \dagger a_{\text{out}}^\mu \rangle\rangle_{\text{ss}}}{|\alpha_\omega^\mu|^2} = 2\beta_\mu - 1 + 2(1 - \beta_\mu) \text{Re}\{\langle\langle t_\omega^\mu \rangle\rangle\} + \mathcal{O}[|\Omega|/\Gamma]^2, \quad (35)$$

with $\beta_\mu = \gamma_\mu/\Gamma$ the directional β -factor, and $\tilde{a}_{\text{out}}^\mu(t) = e^{i\omega t} a_{\text{out}}^\mu(t)$.

Note that, while homodyne measurements in Eq. (34) provide direct access to $\langle\langle t_\omega^\mu \rangle\rangle$, power measurements in Eq. (35) give us only its real part, but we can still reconstruct the full transmittance via the Kramers-Kronig relation,

$$\text{Im}\{\langle\langle t_\omega^\mu \rangle\rangle\} = \frac{1}{\pi} \mathcal{P} \int_{-\infty}^{\infty} d\omega' \frac{1 - \text{Re}\{\langle\langle t_{\omega'}^\mu \rangle\rangle\}}{\omega' - \omega}, \quad (36)$$

with \mathcal{P} representing the Cauchy's principal value of the integral. In the literature it is not well recognized that power measurements alone are enough to determine the modulus and phase of the transmittance $\langle\langle t_\omega^\mu \rangle\rangle$, even in the presence of general correlated noise and dissipation as shown here. Indeed, it is typically believed that power measurements give direct access to $|\langle\langle t_\omega^\mu \rangle\rangle|^2$, but in Appendix D we show that this is only true in the absence of

any dephasing, so that $\text{Re}\{\langle\langle t_\omega^\mu \rangle\rangle\} = |\langle\langle t_\omega^\mu \rangle\rangle|^2$. For more details see [Appendix D](#), which also includes the expressions for single-photon reflectance measurements $\langle\langle r_\omega^\mu \rangle\rangle$, and a discussion on the conservation of the average photon flux in these experiments.

After measuring the single-photon transmittance $\langle\langle t_\omega^\mu \rangle\rangle$, we can invert equation (24) to access to the time-resolved Ramsey envelope $C_\phi(t)$ and characterize noise correlations of the environment. A convenient inverse formula can be derived when the dephasing fluctuation $\Delta(t)$ has a symmetric probability distribution around the average, which is very reasonable assumption in experiments. In this case, the Ramsey envelope defined in Eq. (14) is a real function of time, $C_\phi(t) = [C_\phi(t)]^*$, and it can be directly related to $\text{Re}\langle\langle t_\omega^\mu \rangle\rangle$ by[¶]

$$C_\phi(t) = \sqrt{\frac{2}{\pi}} e^{(\Gamma/2)t} \mathcal{F}^{-1} \left[\frac{1 - \text{Re}\langle\langle t_\omega^\mu \rangle\rangle}{\gamma_\mu} \right] (t), \quad \text{for } t > 0. \quad (37)$$

This relation (37) has important physical consequences to single-photon scattering experiments in waveguide QED, as it demonstrates that applying a Fourier transformation on the usual transmittance data [[3](#), [5](#), [11](#), [59](#), [60](#), [73](#), [74](#)], one can characterize noise correlations without requiring direct access and time-dependent control of the emitter. Moreover, Eq. (37) is particularly convenient in the case of power measurements ([35](#)) as it only requires the knowledge of $\text{Re}\langle\langle t_\omega^\mu \rangle\rangle$, and thus avoids the use of the Kramers-Kronig transformation ([36](#)).

5.2. Derivation of the protocol

Let us briefly summarize how equations ([34](#))-([35](#)) are derived. We begin with the equations of motion for the noisy qubit, taking expectation values on ([6](#))-([7](#)) with the initial condition ([33](#)). Using the property $a_{\text{in}}^\lambda(t) |\Psi(0)\rangle = \alpha_\omega^\mu \delta_{\lambda\mu} e^{-i\omega t} |\Psi(0)\rangle$ with $\lambda = \pm$, and going to a rotating frame with the driving frequency ω , we find

$$\frac{d}{dt} \langle\tilde{\sigma}^-\rangle = - \left(\frac{\Gamma}{2} - i[\omega - \omega_0] + i\Delta(t) \right) \langle\tilde{\sigma}^-\rangle - \Omega \langle\sigma_z\rangle, \quad (38)$$

$$\frac{d}{dt} \langle\sigma_z\rangle = -\Gamma(1 + \langle\sigma_z\rangle) + 2(\Omega^* \langle\tilde{\sigma}^-\rangle + \text{h.c.}). \quad (39)$$

Here, we have defined the slowly evolving coherence $\langle\tilde{\sigma}^-(t)\rangle = e^{i\omega t} \langle\sigma^-(t)\rangle$ and the strength of the coherent drive $\Omega = -i\alpha_\omega^\mu \sqrt{\gamma_\mu}$. The qubit equations are stochastic Bloch equations that can combine correlated dephasing with saturation at strong drives $|\Omega| \gtrsim \Gamma$ [[78](#)]. The stochastic methods from section [Appendix A](#) provide a solution to this complex dynamics of the qubit, but noise spectroscopy only requires the steady state averaged coherence $\langle\langle \langle\tilde{\sigma}^-\rangle \rangle\rangle_{\text{ss}} =$

[¶] Inverting Eq. (24) in the general case leads to $C_\phi(t) = (2\pi)^{-1/2} e^{(\Gamma/2)t} \mathcal{F}^{-1} [(1 - \langle\langle t_\omega^\mu \rangle\rangle)/\gamma_\mu] (t)$, for $t > 0$, but this expression presents a slower numerical convergence compared to Eq. (37). Notice that the presence of a non-zero photon decay $\Gamma > 0$ allows us to mathematically replace the inverse Laplace transform \mathcal{L}^{-1} by the more convenient inverse Fourier transform \mathcal{F}^{-1} .

$\langle\langle\tilde{\sigma}^-\rangle\rangle_{t\rightarrow\infty}$, which appears both in homodyne and power steady state measurements as⁺

$$\frac{\langle\langle\tilde{a}_{\text{out}}^\lambda\rangle\rangle_{\text{ss}}}{\alpha_\omega^\mu} = \delta_{\lambda\mu} - \sqrt{\gamma_\lambda\gamma_\mu}\langle\langle\tilde{\sigma}^-\rangle\rangle_{\text{ss}}/\Omega, \quad (40)$$

$$\frac{\langle\langle a_{\text{out}}^\lambda \dagger a_{\text{out}}^\lambda \rangle\rangle_{\text{ss}}}{|\alpha_\omega^\mu|^2} = \delta_{\lambda\mu} - 2\sqrt{\gamma_\lambda\gamma_\mu} \left(\delta_{\lambda\mu} - \sqrt{\beta_\lambda\beta_\mu} \right) \text{Re} \left\{ \langle\langle\tilde{\sigma}^-\rangle\rangle_{\text{ss}}/\Omega \right\}. \quad (41)$$

In the low driving limit $|\Omega| \ll \Gamma$, the qubit will remain close to the ground state $\langle\sigma_z\rangle = -1 + \mathcal{O}[|\Omega|/\Gamma]^2$, and equations (38) and (21) become equivalent. We can thus map the qubit steady state coherence $\langle\langle\tilde{\sigma}^-\rangle\rangle_{\text{ss}}$ to the solution of average scattering overlap in Sec. 4 as,

$$\langle\langle\tilde{\sigma}^-\rangle\rangle_{\text{ss}}/\Omega = \langle\langle G_\omega \rangle\rangle + \mathcal{O}[|\Omega|/\Gamma]^2. \quad (42)$$

From this relation we conclude that homodyne and power measurements give us full information about the average single-photon transmittance $\langle\langle t_\omega^\mu \rangle\rangle$ and reflectance $\langle\langle r_\omega^\mu \rangle\rangle$, and allow a full spectroscopic characterization of the noise via Eqs. (34)-(37).

6. Conclusions and outlook

We developed a stochastic version of input-output theory which consistently describes the effect of correlated dephasing noise in single-photon scattering experiments with weak coherent inputs. Using this theory, we studied scattering subject to the typical noise models from solid-state and quantum optics —white noise, quasi-static noise, colored Gaussian noise (see Secs. 3.2 and 4.2), and 1/f noise (see Sec. 4.3), in addition to telegraph noise and non-Gaussian jump models in Appendix A—, illustrating how to calculate the single-photon transmittance $\langle\langle t_\omega^\mu \rangle\rangle$ and reflectance $\langle\langle r_\omega^\mu \rangle\rangle$ of each model.

Complementary to these theoretical developments, we introduced a spectroscopic method that extracts the qubit noise correlations from standard homodyne or photon counting measurements. The method provides the same information as time-resolved Ramsey experiments, but does not require direct access or time-dependent control of the emitter. This method and the techniques developed in this work are suited not only for waveguide QED experiments —superconducting circuits [3–5, 15], quantum dots in photonic crystals [59, 60], SiV-centers in diamond waveguides [74, 79], or nanoplasmonics [80]—, but also for generic experiments with two-level quantum emitters interacting with propagating photons, such as molecules in a 3D bath [73] or ions in a Paul trap [81].

There are still several open questions and extensions to consider in the interaction between few photons and noisy quantum emitters. For instance, our theory is valid for general stationary random fluctuations $\Delta(t)$, but we only analyzed phenomenological classical noise models. Therefore, it would be interesting to study the effects of specific microscopic quantum models producing correlated pure dephasing on the quantum scatterers [82, 83], and try to find the connections to the phenomenological models analyzed here. Moreover, we can combine

⁺ To derive the relation (41), we combined the input-output equations (9), the equation of motion (39), and used the exact relation $\langle\langle\sigma_z\rangle\rangle_{\text{ss}} = -1 + \text{Re} \{ 4\Omega^* \langle\langle\tilde{\sigma}^-\rangle\rangle_{\text{ss}}/\Gamma \}$, which results from integrating (39) and averaging in steady state.

the stochastic methods discussed here with our recent theory of scattering tomography [49] to characterize multi-photon processes or many-body scatterers [84–86] under realistic conditions of noise.

Acknowledgments

The authors acknowledge discussions with P. Eder and F. Deppe. This work was supported by the MINECO/FEDER Project FIS2015-70856-P and CAM PRICYT Research Network QUITEMAD+ S2013/ICE-2801. TR further acknowledges the Juan de la Cierva fellowship FJCI-2016-29190.

Appendix A. Average single-photon transmittance of a qubit with dephasing due to correlated non-Gaussian Markovian noise models

In the main text we explicitly calculated the average transmittance of a qubit with colored Gaussian noise and Gaussian 1/f noise, where $C_\phi(t)$ is analytical and $\langle\langle t_\omega^\mu \rangle\rangle$ can be directly obtained from (24). Although Gaussian noise models are very successfully applied in numerous experiments [82], the Gaussianity assumption breaks down in situations where the qubit is coupled to a sparse dephasing environment [38] such as a few frequency modes [58], or ensembles of few two-level fluctuators (TLFs) [63, 70]. In the following we extend the analysis to arbitrary correlated non-Gaussian Markovian noise models which include telegraph noise caused by a single TLF (see Appendix A.2), tunable non-Gaussian noise caused by a sparse ensemble of TLFs (see Appendix A.3), and non-Gaussian 1/f noise (see Appendix A.4) typically found in solid-state devices [28]. To compute $\langle\langle t_\omega^\mu \rangle\rangle$ and $C_\phi(t)$ for a qubit under these types of dephasing, we require the stochastic methods introduced in the following subsection Appendix A.1.

Appendix A.1. Stochastic differential equations with arbitrary correlated Markovian noise

Here we state the equations to solve for the average transmittance $\langle\langle t_\omega^\mu \rangle\rangle$ and the Ramsey envelope $C_\phi(t)$ in the case of the most general correlated, stationary, and Markovian dephasing noise. In practice, we generalize the method in page 418 of Ref. [51] to inhomogeneous stochastic differential equations, and then apply it to the scattering equation (21).

Our first assumption is that the stochastic process $\Delta(t)$ is stationary and Markovian. The probability for the noise to be in realization $\Delta(t) = \Delta$ at time t , conditioned on being $\Delta(t_0) = \Delta_0$ at time t_0 is denoted by $P(\Delta, t) = P(\Delta, t | \Delta_0, t_0)$. The most general Markovian dynamics for the above conditional probability is governed by a differential Chapman-Kolmogorov equation [52],

$$\frac{\partial}{\partial t} P(\Delta, t) = LP(\Delta, t), \tag{A.1}$$

with initial condition $P(\Delta, t_0) = \delta(\Delta - \Delta_0)$ and classical Liouvillian L given by

$$LP(\Delta, t) = -\frac{\partial}{\partial \Delta}[D_1(\Delta)P(\Delta, t)] + \frac{1}{2}\frac{\partial^2}{\partial \Delta^2}[D_2(\Delta)P(\Delta, t)] + \int d\Delta' W(\Delta, \Delta')P(\Delta', t). \quad (\text{A.2})$$

Here, $D_1(\Delta)$ is the drift function, $D_2(t) \geq 0$ the diffusion function, and $W(\Delta, \Delta') \geq 0$ for $\Delta \neq \Delta'$ are transition probabilities between different values of the noise. The conservation of total probability also requires $\int d\Delta LP(\Delta, t) = 0$ and thus $\int d\Delta W(\Delta, \Delta') = 0$. We further assume L is time-independent to have an homogeneous stationary Markovian process with well-defined steady state $LP_{\text{ss}}(\Delta) = 0$.

We want to study $G_\omega(t)$ which is a stochastic process related to $\Delta(t)$ via Eq. (21). Since $\Delta(t)$ is Markovian, the joint process $[\Delta(t), G_\omega(t)]$ is Markovian too [51] with joint probability denoted by $\mathcal{P}(G_\omega, \Delta, t)$. For a multiplicative inhomogeneous stochastic differential equation of the form $dG/dt = A(\Delta)G + B$, the joint probability satisfies [51]

$$\frac{\partial}{\partial t}\mathcal{P}(G_\omega, \Delta, t) = -A(\Delta)\frac{\partial}{\partial G_\omega}(G_\omega\mathcal{P}) - B\frac{\partial \mathcal{P}}{\partial G_\omega} + L\mathcal{P}, \quad (\text{A.3})$$

with the initial condition $\mathcal{P}(G_\omega, \Delta, 0) = \delta(G_\omega - G_\omega(0))P(\Delta, 0)$. To compute the noise average $\langle\langle G_\omega \rangle\rangle$, the strategy is to convert the stochastic equation (21) into a set of ordinary differential equations for the *marginal averages* $g_\omega(\Delta, t) = \int dG_\omega G_\omega \mathcal{P}(G_\omega, \Delta, t)$, and from its solution obtain the total average as $\langle\langle G_\omega \rangle\rangle(t) = \int d\Delta g_\omega(\Delta, t)$. To do so, we insert $A(\Delta) = -[\Gamma/2 - i(\omega - \omega_0) + i\Delta]$ and $B = 1$ in Eq. (A.3), multiply it by G_ω and integrate it over $G_\omega(t)$, obtaining

$$\frac{\partial g_\omega(\Delta, t)}{\partial t} = -[\Gamma/2 - i(\omega - \omega_0) + i\Delta]g_\omega(\Delta, t) + P(\Delta, t) + Lg_\omega(\Delta, t). \quad (\text{A.4})$$

For the scattering problem in Sec. 4.1, the differential equation (A.4) must be solved with the initial condition $g_\omega(\Delta, -\infty) = G_\omega(-\infty)P(\Delta, -\infty) = 0$, which effectively corresponds to finding the steady state solution $g_\omega^{\text{ss}}(\Delta) = g_\omega(\Delta, t \rightarrow \infty)$ or $dg_\omega(\Delta, t)/dt = 0$. Finally, when having the steady state marginal averages $g_\omega^{\text{ss}}(\Delta)$ for each frequency ω and each noise realization Δ , we obtain the average transmittance as

$$\langle\langle t_\omega^\mu \rangle\rangle = 1 - \gamma_\mu \int d\Delta g_\omega^{\text{ss}}(\Delta). \quad (\text{A.5})$$

We see that computing the average transmittance $\langle\langle t_\omega^\mu \rangle\rangle$ for the most general non-Gaussian, correlated, stationary, and Markovian noise model amounts to solve for the steady state of the partial differential equation (A.4) and then to integrate it in Eq. (A.5) over all noise realizations.

To simplify the above solution, we now particularize the analysis to discrete jump noise models, where the stochastic process $\Delta(t)$ has a discrete number of realizations denoted by Δ_m . In this case, we can set $D_1 = D_2 = 0$ in Eq. (A.2), and the probability $P(\Delta_m, t)$ for the noise to be in the realization $\Delta(t) = \Delta_m$ at time t , conditioned on being $\Delta(t_0) = \Delta_{m_0}$ at $t = t_0$ is governed by the time-local rate equation [51],

$$\frac{d}{dt}P(\Delta_m, t) = LP(\Delta_m, t) = \sum_n W_{mn}P(\Delta_n, t). \quad (\text{A.6})$$

Here, the matrix coefficients $W_{mn} \geq 0$ for $m \neq n$ describe transition rates of the noise to jump from realization Δ_n to Δ_m —which must satisfy $\sum_m W_{mn} = 0$ to ensure the conservation of total probability $\sum_m P(\Delta_m, t) = 1$ —. Importantly, the partial differential equation (A.4) reduces to a discrete set of ordinary differential equations for the discrete number of marginal averages $g_\omega(\Delta_m, t)$ as,

$$\frac{d}{dt}g_\omega(\Delta_m, t) = -\left(\frac{\Gamma}{2} - i[\omega - \omega_0] + i\Delta_m\right)g_\omega(\Delta_m, t) + P(\Delta_m, t) + \sum_n W_{mn}g_\omega(\Delta_n, t), \quad (\text{A.7})$$

which now allows us for a much simpler steady state solution. In fact, setting $dg_\omega(\Delta_m, t)/dt = 0$ in Eq. (A.7) we can map the problem to a linear system of equations,

$$\sum_n J_{mn}g_\omega^{\text{ss}}(\Delta_n) = P_{\text{ss}}(\Delta_m), \quad \text{with} \quad (\text{A.8})$$

$$J_{mn} = [\Gamma/2 - i(\omega - \omega_0) + i\Delta_m]\delta_{mn} - W_{mn}. \quad (\text{A.9})$$

Here, the matrix J_{mn} is of the same size as W_{mn} , and $P_{\text{ss}}(\Delta_m)$ denotes the steady state solution of the rate equations (A.6). Finally, solving this linear problem for different values of the input field ω , we obtain the average single-photon transmittance from the sum,

$$\langle\langle t_\omega^\mu \rangle\rangle = 1 - \gamma_\mu \sum_m g_\omega^{\text{ss}}(\Delta_m). \quad (\text{A.10})$$

On the other hand, to obtain the Ramsey envelope $C_\phi(t)$ in Eq. (14), we can numerically extract it from $\langle\langle t_\omega^\mu \rangle\rangle$ via the inversion formula (37). Alternatively, we can also obtain it by calculating the average solution $C_\phi(t) = \langle\langle X(t) \rangle\rangle$ of the homogeneous stochastic differential equation,

$$\frac{d}{dt}X(t) = -i\Delta(t)X(t). \quad (\text{A.11})$$

A set of differential equations for the marginal averages $x(\Delta_m, t) = \int dX \mathcal{P}(X, \Delta_m, t)X$ can be derived from Eq. (A.3) with $A(\Delta) = -i\Delta$, $B = 0$, and the discrete rate equations (A.6),

$$\frac{d}{dt}x(\Delta_m, t) = -i\Delta_m x(\Delta_m, t) + \sum_n W_{mn}x(\Delta_n, t), \quad (\text{A.12})$$

which must be solved for the initial condition $x(\Delta_m, 0) = P_{\text{ss}}(\Delta_m)$. Finally, we obtain the Ramsey envelope as $C_\phi(t) = \langle\langle X(t) \rangle\rangle = \sum_m x(\Delta_m, t)$.

In the following three subsections, we evaluate $\langle\langle t_\omega^\mu \rangle\rangle$ and $C_\phi(t)$ for different forms and sizes of W_{mn} corresponding to correlated telegraph noise, and more general non-Gaussian 1/f noise models.

Appendix A.2. Telegraph correlated noise

Charges or impurities in the materials of solid-state devices are modeled in many cases as localized double-well potentials or two-level fluctuators (TLFs) [28, 63, 87, 88]. A strong resonant coupling between the qubit and an environmental TLS can lead to the observation of resonances [40, 89, 90], but a weak off-resonant coupling can induce fluctuating Stark shifts

on the qubit and thus originate correlated dephasing as in Eq. (2). Although TLFs naturally appear in large ensembles of them [68–70], the *telegraph noise* produced by a single TLS is an instructive and exactly solvable model capturing many features of more complex correlated non-Gaussian noises.

Telegraph noise is the simplest jump model, where random variable $\Delta(t)$ can only take two possible values $\Delta_{\pm} = \pm\sigma$ [50, 52], corresponding to an increase or decrease of the qubit resonance as $\omega_0 \pm \sigma$. The dynamics of this noise consists in random jumps with rate κ between the two possible realizations Δ_m with $m = \pm$, as depicted in Figure A1(a). The probabilities $P(\Delta_m, t)$ of being in Δ_m at time t , conditioned of being in Δ_{m_0} at an initial time t_0 , are governed by the Markovian rate equations,

$$\frac{d}{dt}P(\Delta_m, t) = -\frac{\kappa}{2}P(\Delta_m, t) + \frac{\kappa}{2}P(\Delta_{-m}, t), \quad (\text{A.13})$$

which can be recast in the general form (A.6) with the transition matrix $W_{mn} = -mn\kappa/2$ ($m, n = \pm$). The above equations imply that in steady state the probabilities of being in either realization are equal $P_{\text{ss}}(\Delta_m) = 1/2$, the mean fluctuation vanishes $\langle\langle\Delta(t)\rangle\rangle = 0$, and the autocorrelation has the same form $\langle\langle\Delta(0)\Delta(\tau)\rangle\rangle = \sigma^2 e^{-\kappa|\tau|}$ [50, 52] as the colored Gaussian noise in Eq. (16). Notice that this is just a coincidence since higher order correlations highly differ due to the non-Gaussian character of the telegraph noise [52].

The simplicity of the telegraph noise allows us to analytically solve for the average transmittance $\langle\langle t_{\omega}^{\mu} \rangle\rangle$ in Eq. (A.10), since the linear system (A.8) is of size 2-by-2 with the matrix $J_{mn} = [\Gamma/2 - i(\omega - \omega_0) + im\sigma]\delta_{mn} + mn\kappa/2$ ($m, n = \pm$), and $P_{\text{ss}}(\Delta_m) = 1/2$. For the steady state marginal averages we obtain

$$g_{\omega}^{\text{ss}}(\Delta_m) = \frac{(\Gamma/2 - i[\omega - \omega_0] + \kappa - im\sigma)}{2[(\Gamma/2 - i[\omega - \omega_0] + \kappa/2)^2 + \sigma^2 - \kappa^2/4]}, \quad (\text{A.14})$$

and using Eq. (A.10) we find that $\langle\langle t_{\omega}^{\mu} \rangle\rangle$ can be expressed in a form reminiscent to a Lorentzian, $\langle\langle t_{\omega}^{\mu} \rangle\rangle = 1 - \gamma_{\mu}/[\Gamma/2 + \gamma_{\phi}(\omega) - i(\omega - \omega_0)]$, but with a frequency-dependent pure dephasing rate $\gamma_{\phi}(\omega)$ given by

$$\gamma_{\phi}(\omega) = \frac{\sigma^2}{\Gamma/2 + \kappa - i(\omega - \omega_0)}. \quad (\text{A.15})$$

The lineshape is thus not Lorentzian in general, except for the white noise limit, ($\kappa, \sigma \rightarrow \infty$ with σ^2/κ constant) where the dephasing rate (A.15) becomes the constant $\gamma_{\phi}(\omega) = \sigma^2/\kappa$. This is illustrated by the blue/solid transmittance in Fig. A1(b) for standard waveguide QED parameters. For a finite but moderate correlation time $\sigma \lesssim \kappa < \infty$, $\langle\langle t_{\omega}^{\mu} \rangle\rangle$ gets broader than the Lorentzian (black/dash-dotted), and in the quasi-static limit of long correlation times $\kappa \ll \sigma < \infty$, $\langle\langle t_{\omega}^{\mu} \rangle\rangle$ develops two well separated dips centered at $\omega \approx \omega_0 \pm \sigma$ whose widths are proportional to σ (red/dashed).

To obtain the Ramsey envelope $C_{\phi}(t)$ for the qubit under this telegraph noise, we can either use the inverse relation Eq. (37) on our known $\langle\langle t_{\omega}^{\mu} \rangle\rangle$ or solve the differential Eq. (A.12), which gives

$$C_{\phi}(t) = \frac{1}{2} [(1 + v_0)e^{v_+ t} + (1 - v_0)e^{v_- t}], \quad (\text{A.16})$$

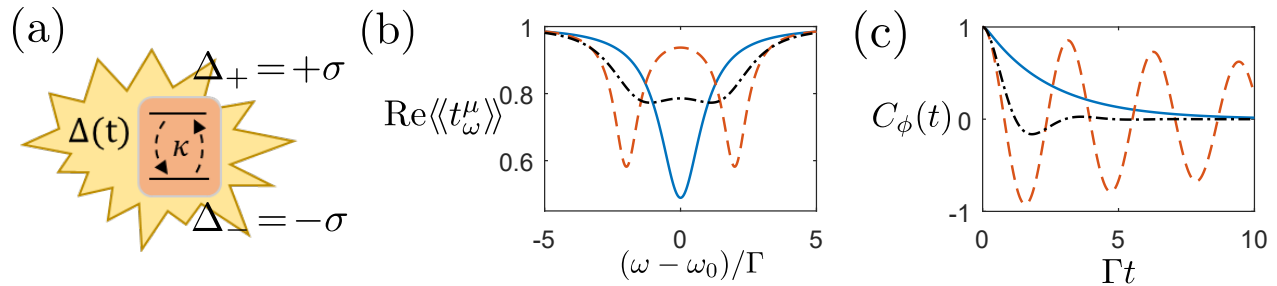


Figure A1. Single-photon scattering on a noisy qubit with random telegraph dephasing. (a) Scheme of two-level fluctuator (TLF) randomly changing the qubit resonance as $\omega_0 \pm \sigma$ with a rate κ . (b) Predictions for the average transmittance $\langle\langle t_\omega^\mu \rangle\rangle$ for $\kappa = 5\sigma$ (white noise, blue/solid), $\kappa = \sigma$ (black/dash-dotted), and $\kappa = 0.05\sigma$ (quasi-static, red/dashed). Other parameters are $\sigma = 2\Gamma$, $\gamma_\pm = \gamma/2$, $\gamma = 0.9\Gamma$, and $\gamma_{\text{loss}} = 0.1\Gamma$. (c) Time-resolved Ramsey envelope $C_\phi(t)$ corresponding to the same parameters and same line-types as in (b).

with $v_0 = \kappa/\sqrt{\kappa^2 - 4\sigma^2}$ and $v_\pm = (-\kappa \pm \sqrt{\kappa^2 - 4\sigma^2})/2$ [51]. As shown in Figure A1(c), $C_\phi(t)$ is the exponential decay in the white noise limit, and for a finite correlation time $\kappa < \infty$, it shows damped oscillations with frequency $\sim \sigma$ and damping rate $\sim \kappa$.

Appendix A.3. Correlated dephasing noise with tunable non-Gaussianity

In this subsection we introduce a model of non-Gaussian correlated noise, whose non-Gaussianity can be tuned to describe situations such as the telegraph noise from previous subsection, all the way to the limit of colored Gaussian noise in Secs. 3.2 and 4.2.

We follow Ref. [91] and construct a discrete noise model from the sum of M independent and identical TLFs, $\Delta(t) = \sum_{i=1}^M \Delta_i(t)/\sqrt{M}$ (see Figure A2(a)). Here, each noise component $\Delta_i(t)$ corresponds to a telegraph noise as in the previous subsection, which flips between the values $\Delta_i(t) = \pm\sigma$ at a rate κ and independently satisfies the Markovian rate equation (A.13). Since all noise components are identical and uncorrelated, the autocorrelation of the total noise $\Delta(t)$ coincides with the one of a single telegraph noise $\langle\langle \Delta(0)\Delta(\tau) \rangle\rangle = \sigma^2 e^{-\kappa|\tau|}$, but higher order moments strongly depend on M . Due to the permutation symmetry of the dephasing environment, there are $M + 1$ distinguishable realizations Δ_m of the total noise, labeled by $m = 0, \dots, M$, and given by

$$\Delta_m = \frac{(2m - M)}{\sqrt{M}}\sigma. \quad (\text{A.17})$$

For instance, the realization $\Delta_0 = -\sigma/\sqrt{M}$ corresponds to the configuration with all TLFs down, which vary all the way to $\Delta_M = \sigma/\sqrt{M}$ where all TLFs are up. A given realization Δ_m appears in the environment with a multiplicity $\binom{M}{m} = M!/[(M - m)!m!]$, and thus the probability $P(\Delta_m, t)$ to find the global realization Δ_m at time t can be related to the probabilities of a single telegraph noise $P(\Delta_\pm, t)$ by

$$P(\Delta_m, t) = \binom{M}{m} [P(\Delta_-, t)]^{M-m} [P(\Delta_+, t)]^m, \quad \text{with } m = 0, \dots, M. \quad (\text{A.18})$$

Using Eqs. (A.13) and (A.18), we can derive the rate equation for $P(\Delta_m, t)$, which takes the general form in Eq. (A.6), with a transition matrix W_{nm} whose nonzero elements read [91],

$$W_{mm} = -\frac{M}{2}\kappa, \quad W_{m,m+1} = \frac{\kappa}{2}(m+1), \quad W_{m,m-1} = \frac{\kappa}{2}(M+1-m), \quad (\text{A.19})$$

for $m = 0, \dots, M$, and the boundary conditions $P(\Delta_{-1}, t) = P(\Delta_{M+1}, t) = 0$.

The steady state solution of the rate equation (A.6) with the W_{mn} coefficients (A.19) is a binomial distribution $P_{\text{ss}}(\Delta_m) = \frac{1}{2^M} \binom{M}{m}$ as can also be seen by setting $P_{\text{ss}}(\Delta_{\pm}) = 1/2$ in Eq. (A.18). Importantly, in the limit of an infinitely large ensemble of TLFs, $M \rightarrow \infty$, the binomial probability distribution $P_{\text{ss}}(\Delta_m)$ approaches a continuous Gaussian distribution $P_{\text{G}}(\Delta) = (2\pi\sigma^2)^{-1/2} e^{-\Delta^2/(2\sigma^2)}$ as $P_{\text{ss}}(\Delta_m) = P_{\text{G}}(\Delta) d\Delta [1 + \mathcal{O}(M^{-1/2})]$ and we recover the colored Gaussian noise limit of Secs. 3.2 and 4.2. In fact, in the limit $M \rightarrow \infty$, the rate equation (A.6) with (A.19) becomes a continuous Fokker-Planck differential equation for the Ornstein-Uhlenbeck process [91], which is given by Eqs. (A.1)-(A.2) with $D_1(\Delta) = -\kappa\Delta$, $D_2 = 2\kappa\sigma^2$, and $W(\Delta, \Delta') = 0$. As a result of this connection, we conclude that by increasing the number M of independent telegraph noises, we can reduce the non-Gaussian character of the noise model until reaching the limit of standard colored Gaussian noise.

We exemplify this tuning of the non-Gaussianity by computing the average transmittance $\langle\langle t_{\omega}^{\mu} \rangle\rangle$ for a qubit in dephasing environments with different values of M . To do so, we numerically solve the linear system (A.8)-(A.9) by using the W_{mn} coefficients in Eq. (A.19), and the steady state binomial distribution $P_{\text{ss}}(\Delta_m) = \frac{1}{2^M} \binom{M}{m}$. It is computationally simple to reach the Gaussian limit $M \gg 1$ since the size of the matrix J_{mn} grows linearly with M as $(M+1) \times (M+1)$. The results are shown in Figure A2(b) for $M = [2, 3, 4, 5, 10]$, $\kappa = 0.1\sigma$, and typical waveguide QED parameters. The non-Gaussianity of the dephasing is manifested by the multiple dips in $\langle\langle t_{\omega}^{\mu} \rangle\rangle$ which reduce with increasing M . Also notice that already for $M = 10$ (red/dashed) the Gaussian limit is well-established with a Gaussian-like transmittance as expected in the quasi-static limit $\kappa \ll \sigma < \infty$. In addition, we compute the Ramsey envelopes $C_{\phi}(t)$ for the parameters above by applying Eq. (37) on the numerical data for $\langle\langle t_{\omega}^{\mu} \rangle\rangle$. The results are shown in Figure A2(c), where the non-Gaussianity of the dephasing noise is manifested by the multiple oscillations in $C_{\phi}(t)$ and whose amplitude reduce with M . In the Gaussian limit (red/dashed) there is only the Gaussian decay as expected in the quasi-static case $\kappa = 0.1\sigma$. Notice that we do not display the results in the white noise limit, where the behavior is independent of M , the lineshapes are standard Lorentzians, and $C_{\phi}(t)$ are exponential decays with pure dephasing rate $\gamma_{\phi} = \sigma^2/\kappa$.

Appendix A.4. Simulation of non-Gaussian 1/f noise

The aim of this subsection is to construct a model for 1/f noise with tunable non-Gaussianity and show how to compute the non-Gaussian results for $\langle\langle t_{\omega}^{\mu} \rangle\rangle$ in Figure 4(b)-(c). To simulate non-Gaussian 1/f noise, we assume that each noise component $\Delta_j(t)$ for $j = 1, \dots, N$ in Eq. (29) is represented by an independent ensemble of M identical TLFs as introduced in Appendix A.3. We therefore need to construct a more general jump model for the total

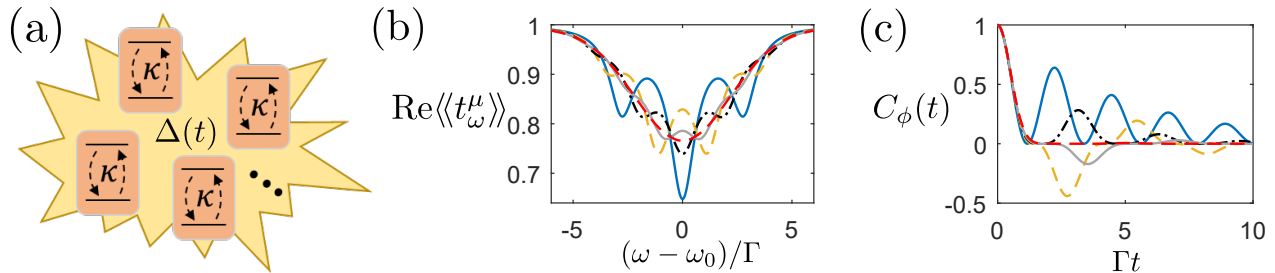


Figure A2. Noisy qubit with non-Gaussian noise due to an ensemble of M identical and independent two-level fluctuators (TLFs). (a) Scheme of the dephasing environment, characterized by jumps at rate κ and an average noise amplitude σ . (b) Average transmittance $\langle\langle t_\omega^\mu \rangle\rangle$ for $M = [2, 3, 4, 5, 10]$ (blue, orange, black, grey, red), and the parameters $\kappa = 0.1\sigma$, $\sigma = 2\Gamma$, $\gamma_\pm = \gamma/2$, $\gamma = 0.9\Gamma$, and $\gamma_{\text{loss}} = 0.1\Gamma$. (c) Time-resolved Ramsey envelope $C_\phi(t)$ corresponding to the same parameters and same line-types as in (b).

noise, $\Delta(t) = \sum_{j=1}^N \Delta_j(t)/\sqrt{N}$, with permutation symmetry only within each ensemble $\Delta_j(t)$. As a result, there will be $(M+1)^N$ distinguishable global realizations of the total noise $\Delta(t)$, which are given by

$$\Delta_{\vec{m}} = \sum_{j=1}^N \frac{(2m_j - M)}{\sqrt{M}} \sigma_j. \quad (\text{A.20})$$

Here, we use the vectorial index $\vec{m} = (m_1, \dots, m_N)$, with components $m_j = 0, \dots, M$, to label the above $(M+1)^N$ different realizations $\Delta_{\vec{m}}$. Then, by straightforwardly generalizing the procedure in [Appendix A.3](#), one can show that probability $P(\Delta_{\vec{m}}, t)$ satisfies a rate equation of the form [\(A.6\)](#), with a transition matrix $W_{\vec{m}\vec{n}}$ of size $(M+1)^N \times (M+1)^N$ and nonzero matrix elements given by,

$$W_{\vec{m}\vec{m}} = -\frac{M}{2} \sum_{j=1}^N \kappa_j, \quad W_{\vec{m}, \vec{m} + \vec{e}_j} = \frac{\kappa_j}{2} (m_j + 1), \quad W_{\vec{m}, \vec{m} - \vec{e}_j} = \frac{\kappa_j}{2} (M + 1 - m_j), \quad (\text{A.21})$$

where $\vec{e}_j = (0, \dots, 1_j, \dots, 0)$ is a unit vector in component $j = 1, \dots, N$. Solving the corresponding rate equation with boundary conditions $P(\Delta_{\vec{m}}, t) = 0$ for $m_j = -1, M+1$, and $j = 1, \dots, N$, we find that the steady state probability $P_{\text{ss}}(\Delta_{\vec{m}})$ corresponds to a product of binomial distributions for each $\Delta_j(t)$, which reads

$$P_{\text{ss}}(\Delta_{\vec{m}}) = \frac{1}{2^{NM}} \prod_{j=1}^N \binom{M}{m_j}. \quad (\text{A.22})$$

Finally, we should evaluate $W_{\vec{m}\vec{n}}$ for the parameters κ_j and σ_j that simulate the desired 1/f noise model as stated in [Sec. 4.3](#), replace this and [Eq. \(A.22\)](#) in the linear system [\(A.8\)](#)-[\(A.9\)](#), and numerically solve for the steady state marginal averages. With that result we can evaluate $\langle\langle t_\omega^\mu \rangle\rangle$ via [Eq. \(A.10\)](#), and $C_\phi(t)$ via [Eq. \(37\)](#). The size of the linear system scales exponentially with N as $(M+1)^N$, but as shown in [Figure 4\(a\)](#), already a moderate $N = 8$ is enough to properly simulate the 1/f noise spectrum.

Appendix B. Correlated dephasing noise in a qubit with Fano resonance

Some waveguide QED experiments are affected by input-output impedance mismatches or internal reflections that impose a Fano resonance profile on the scattering experiment [59,60]. We briefly discuss how to modify our protocol and the scattering equations for reconstructing the power measurements and the noise correlations in such complex environments.

Following Refs. [59,60,77], we see that a Fano resonance can be modeled by a highly dissipative cavity mode that mediates the coupling between the propagating photons and the qubit. In this case, the cavity mode can be adiabatically eliminated [77] and the effective dynamics of the qubit is governed by quantum Langevin equations with the same form as Eqs. (6)-(7), but with a modified total decay $\Gamma \rightarrow \gamma_{\text{loss}} + \text{Re}\{z_\omega\}\gamma$, a modified qubit central frequency $\omega_0 \rightarrow \omega_0 + \text{Im}\{z_\omega\}\gamma/2$, and a modified input operator $a_{\text{in}}^\mu(t) \rightarrow z_\omega a_{\text{in}}^\mu(t)$. The correction z_ω is the Fano resonance function, which depends on the frequency of the incident photon ω and is given by

$$z_\omega = \frac{1}{1 - 2i(\omega - \omega_c)/\kappa}, \quad (\text{B.1})$$

with ω_c the resonance frequency and κ the decay of the localized mode producing the Fano resonance. In addition, the input-output relations (9) are modified as [77]

$$a_{\text{out}}^\mu(t) = \sum_\lambda \Lambda_{\mu\lambda}(\omega) a_{\text{in}}^\lambda(t) + iz_\omega \sqrt{\gamma_\mu} \sigma^-(t), \quad (\text{B.2})$$

with coefficients $\Lambda_{\mu\lambda}(\omega) = \delta_{\mu\lambda} - 2z_\omega \sqrt{\gamma_\mu \gamma_\lambda} / \gamma$, and the indices $\mu, \lambda = \pm$ corresponding to photons propagating to the right (+) and left (-) of the waveguide.

Appendix B.1. Single-photon scattering matrix of a noisy qubit with Fano resonance

From the modified Langevin equations and input-output relation stated above, we can calculate the average single-photon scattering matrix $\langle\langle S_{\nu\omega}^{\lambda\mu} \rangle\rangle_{\text{Fano}}$ for a qubit with Fano resonance, using the same procedure and definitions shown in Sec. (4.1). We obtain,

$$\langle\langle S_{\nu\omega}^{\lambda\mu} \rangle\rangle_{\text{Fano}} = \{ \Lambda_{\mu\lambda}(\omega) + z_\omega \sqrt{\gamma_\lambda \gamma_\mu} \langle\langle G_\omega \rangle\rangle_{\text{Fano}} \} \delta(\nu - \omega), \quad (\text{B.3})$$

with

$$\langle\langle G_\omega \rangle\rangle_{\text{Fano}} = \mathcal{L}[C_\phi(t)] ([z_\omega \gamma + \gamma_{\text{loss}}]/2 - i[\omega - \omega_0]). \quad (\text{B.4})$$

The average single-photon transmittance and reflectance in the presence of correlated noise then read,

$$\langle\langle t_\omega^\mu \rangle\rangle_{\text{Fano}} = 1 - \frac{z_\omega \gamma_\mu}{\gamma/2} + z_\omega \gamma_\mu \langle\langle G_\omega \rangle\rangle_{\text{Fano}}, \quad \langle\langle r_\omega^\mu \rangle\rangle_{\text{Fano}} = -\frac{z_\omega \sqrt{\gamma_+ \gamma_-}}{\gamma/2} \left(1 - \frac{\gamma}{2} \langle\langle G_\omega \rangle\rangle_{\text{Fano}} \right). \quad (\text{B.5})$$

Notice that in the case of an exact Fano resonance ($\omega_c = \omega$), the qubit effectively behaves as it would be directly coupled to two independent waveguides on each side as treated in Refs. [1,92]. This situation is known as a “direct-coupled” qubit in contrast to the “side-coupled” qubit we consider throughout the main text. It is discussed in Refs. [1,92] that the

results of both cases are related, up to a phase, by interchanging the roles of transmission and reflection. Here, by setting $z_\omega = 1$ in Eqs. (B.5), and considering a non-chiral case $\gamma_\mu = \gamma/2$, we find that these relations are still valid in the presence of correlated noise, namely $\langle\langle t_\omega^\mu \rangle\rangle_{\text{Fano}} = -\langle\langle r_\omega^\mu \rangle\rangle$, and $\langle\langle r_\omega^\mu \rangle\rangle_{\text{Fano}} = -\langle\langle t_\omega^\mu \rangle\rangle$.

Appendix B.2. Power and homodyne measurements of a noisy qubit with Fano resonance

Using the replacements $\Gamma \rightarrow \gamma_{\text{loss}} + \text{Re}\{z_\omega\}\gamma$, $\omega_0 \rightarrow \omega_0 + \text{Im}\{z_\omega\}\gamma/2$, and $\Omega \rightarrow z_\omega\Omega$ in the optical Bloch equations (38)-(39), we can generalize Eqs. (34)-(36) and (D.1)-(D.3) for the homodyne or power measurements, and obtain

$$\frac{\langle\langle a_{\text{out}}^\lambda \rangle\rangle_{\text{ss}}}{\alpha_\omega^\mu} = \Lambda_{\mu\lambda}(\omega) + z_\omega^2 \sqrt{\gamma_\mu \gamma_\lambda} \langle\langle Q_\omega \rangle\rangle, \quad (\text{B.6})$$

$$\frac{\langle\langle a_{\text{out}}^\lambda \dagger a_{\text{out}}^\lambda \rangle\rangle_{\text{ss}}}{|\alpha_\omega^\mu|^2} = |\Lambda_{\mu\lambda}(\omega)|^2 + 2\sqrt{\gamma_\mu \gamma_\lambda} \text{Re}\{\mathcal{K}_{\mu\lambda}(\omega)\langle\langle Q_\omega \rangle\rangle\}, \quad (\text{B.7})$$

$$\text{Im}\{\mathcal{K}_{\mu\lambda}(\omega)\langle\langle Q_\omega \rangle\rangle\} = -\frac{1}{\pi} \mathcal{P} \int_{-\infty}^{\infty} d\omega' \frac{\text{Re}\{\mathcal{K}_{\mu\lambda}(\omega')\langle\langle Q_{\omega'} \rangle\rangle\}}{\omega' - \omega}. \quad (\text{B.8})$$

Here, $\langle\langle Q_\omega \rangle\rangle = \langle\langle \sigma^- \rangle\rangle_{\text{ss}}/\Omega$, and the coefficients $\mathcal{K}_{\mu\lambda}(\omega)$ read

$$\mathcal{K}_{\mu\lambda}(\omega) = z_\omega^2 \Lambda_{\mu\lambda}^*(\omega) + \frac{|z_\omega|^4 \sqrt{\gamma_\mu \gamma_\lambda}}{(|z_\omega|^2 \gamma + \gamma_{\text{loss}})}. \quad (\text{B.9})$$

The new equations (B.6)-(B.7) are valid for measuring at both the transmission ($\lambda = \mu$) and the reflection ($\lambda = -\mu$) output, and provide a robust method to infer $\langle\langle Q_\omega \rangle\rangle$, which is related to the average scattering overlap $\langle\langle G_\omega \rangle\rangle_{\text{Fano}}$ in Eq. (B.4) as

$$\langle\langle Q_\omega \rangle\rangle = \langle\langle G_\omega \rangle\rangle_{\text{Fano}} + \mathcal{O}[|\Omega|/\Gamma]^2, \quad (\text{B.10})$$

in the limit $|\Omega| \ll \Gamma$. Using Eqs. (B.7)-(B.10) we can experimentally determine $\langle\langle G_\omega \rangle\rangle_{\text{Fano}}$ and from there obtain the single-photon transmission and reflection coefficients (B.5), in the case of a Fano resonance. Finally, from the knowledge of $\langle\langle G_\omega \rangle\rangle_{\text{Fano}}$ we can also invert Eq. (B.4), in analogy to Eq. (37), and recover the Ramsey profile from the above spectroscopic measurements as

$$C_\phi(t) = \frac{1}{2\pi} e^{\gamma_{\text{loss}} t/2} \mathcal{F}^{-1} [e^{z_\omega \gamma t/2} \langle\langle G_\omega \rangle\rangle_{\text{Fano}}] (t), \quad \text{for } t > 0, \quad (\text{B.11})$$

where we can use \mathcal{F}^{-1} instead of \mathcal{L}^{-1} due to the non-zero emission rates into guided γ or unguided γ_{loss} modes.

Appendix C. Adding a white noise background to the dephasing model

In this appendix, we use stochastic Ito calculus [50, 52] to include dephasing due to a white noise background $\Delta_{\text{WB}}(t)$, in addition to the correlated noise $\Delta(t)$ in the scattering differential equation (21).

The stochastic differential equation for scattering that includes both noise sources reads,

$$\frac{d}{dt} G_\omega(t) = - \left(\frac{\Gamma}{2} - i[\omega - \omega_0] + i[\Delta(t) + \Delta_{\text{WB}}(t)] \right) G_\omega(t) + 1, \quad (\text{C.1})$$

where the white noise background is specified by the autocorrelation function $\langle\langle \Delta_{\text{WB}}(0)\Delta_{\text{WB}}(\tau) \rangle\rangle = 2\gamma_{\text{WB}}\delta(\tau)$, with γ_{WB} its pure dephasing rate. The multiplicative stochastic differential equation (C.1) must be physically interpreted in the Stratonovich form [50, 52],

$$(S) \quad dG_\omega(t) = - \left(\frac{\Gamma}{2} - i[\omega - \omega_0] + i\Delta(t) \right) G_\omega(t)dt + dt + i\sqrt{2\gamma_{\text{WB}}}G_\omega(t)dW(t), \quad (C.2)$$

with $dW(t) = \Delta_{\text{WB}}(t)dt/\sqrt{2\gamma_{\text{WB}}}$ the Wiener increment. To solve the average over the white noise background more easily, we use the Ito rules to convert Eq. (C.2) to the Ito form, obtaining

$$(I) \quad dG_\omega(t) = - \left(\frac{\Gamma}{2} + \gamma_{\text{WB}} - i[\omega - \omega_0] + i\Delta(t) \right) G_\omega(t)dt + dt + i\sqrt{2\gamma_{\text{WB}}}G_\omega(t)dW(t), \quad (C.3)$$

where now $dW(t)$ is uncorrelated with $G_\omega(t)$ at equal times. We take the average over the white noise background $\langle\langle \dots \rangle\rangle_{\text{WB}}$, which does not affect $\Delta(t)$ as we assume it is uncorrelated with $\Delta_{\text{WB}}(t)$, i.e. $\langle\langle \Delta(t)\Delta_{\text{WB}}(t) \rangle\rangle_{\text{WB}} = 0$ and $\langle\langle \Delta(t)G_\omega(t) \rangle\rangle_{\text{WB}} = \Delta(t)\langle\langle G_\omega(t) \rangle\rangle_{\text{WB}}$. Additionally using the Ito property $\langle\langle G_\omega(t)dW(t) \rangle\rangle_{\text{WB}} = \langle\langle G_\omega(t) \rangle\rangle_{\text{WB}}\langle\langle dW(t) \rangle\rangle_{\text{WB}} = 0$, we obtain a stochastic differential equation that depends on the correlated noise $\Delta(t)$ only,

$$\frac{d}{dt}\langle\langle G_\omega \rangle\rangle_{\text{WB}} = - \left(\frac{\Gamma}{2} + \gamma_{\text{WB}} - i[\omega - \omega_0] + i\Delta(t) \right) \langle\langle G_\omega \rangle\rangle_{\text{WB}}(t) + 1. \quad (C.4)$$

Therefore, we can solve this stochastic differential equation instead of (21) if we would like to include an extra uncorrelated white noise background with pure dephasing rate γ_{WB} . In practice it just amounts to perform the replacement $\Gamma/2 \rightarrow \Gamma/2 + \gamma_{\text{WB}}$ in Eq. (21), before starting to solve it.

Appendix D. Measurement of single-photon reflectance and conservation of average photon flux

In this appendix we complement the analysis from section 5, providing formulas for the average reflectance $\langle\langle r_\omega^\mu \rangle\rangle$, and a word of caution on the interpretation of the squares of the averages $|\langle\langle r_\omega^\mu \rangle\rangle|^2$ and $|\langle\langle t_\omega^\mu \rangle\rangle|^2$, in the presence of dephasing.

The average single-photon transmittance $\langle\langle t_\omega^\mu \rangle\rangle$ can be measured via Eqs. (34)-(36) in Sec. 5 when performing homodyne or power measurements at the output of the same channel $\mu = \pm$ as the weak input drive α_ω^μ . If we instead perform the measurements at the opposite channel $\lambda = -\mu$, we access to the average reflectance $\langle\langle r_\omega^\mu \rangle\rangle$ via the relations,

$$\frac{\langle\langle \tilde{a}_{\text{out}}^{(-\mu)}(t) \rangle\rangle_{\text{ss}}}{\alpha_\omega^\mu} = \langle\langle r_\omega^\mu \rangle\rangle + \mathcal{O} [|\Omega|/\Gamma]^2, \quad (D.1)$$

$$\frac{\langle\langle a_{\text{out}}^{(-\mu)\dagger}(t)a_{\text{out}}^{(-\mu)}(t) \rangle\rangle_{\text{ss}}}{|\alpha_\omega^\mu|^2} = -2\sqrt{\beta_\lambda\beta_\mu}\text{Re}\{\langle\langle r_\omega^\mu \rangle\rangle\} + \mathcal{O} [|\Omega|/\Gamma]^2, \quad (D.2)$$

$$\text{Im}\{\langle\langle r_\omega^\mu \rangle\rangle\} = -\frac{1}{\pi}\mathcal{P} \int_{-\infty}^{\infty} d\omega' \frac{\text{Re}\{\langle\langle r_{\omega'}^\mu \rangle\rangle\}}{\omega' - \omega}. \quad (D.3)$$

When a quantum emitter is affected by dephasing, the squares of the average transmittance and reflectances do not add to one. This is because the dephasing environment exerts work, adding and subtracting energy on the qubit in order to change its transition frequency. For stationary noise the average work is zero, but still the system of qubit and photons is open due to the external stochastic field $\Delta(t)$. In the simple case of white noise dephasing, we can evaluate Eqs. (25) and (27) and obtain

$$|\langle\langle t_\omega^\mu \rangle\rangle|^2 + |\langle\langle r_\omega^\mu \rangle\rangle|^2 + |\langle\langle r_\omega^{\mu, \text{loss}} \rangle\rangle|^2 = 1 - \frac{\gamma_\phi \gamma_\mu}{(\Gamma/2 + \gamma_\phi)^2 + (\omega - \omega_0)^2}, \quad (\text{D.4})$$

with $\langle\langle r_\omega^{\mu, \text{loss}} \rangle\rangle = \sqrt{\gamma_{\text{loss}}/\gamma_\mu} (\langle\langle t_\omega^\mu \rangle\rangle - 1)$ the fluorescence reflectance into unguided modes, and γ_ϕ the pure dephasing rate.

This means that the squares of the average transmittance or reflectance do not describe photon fluxes when $\gamma_\phi \neq 0$. The noisy qubit indeed conserves the total photon flux on average, in the case of stationary dephasing, but this is manifested in the sum of the average output power in all channels, i.e. transmission, reflection, and fluorescence loss, as

$$\frac{\langle\langle a_{\text{out}}^{\mu \dagger}(t) a_{\text{out}}^\mu(t) \rangle\rangle_{\text{ss}}}{|\alpha_\omega^\mu|^2} + \frac{\langle\langle a_{\text{out}}^{(-\mu) \dagger}(t) a_{\text{out}}^{(-\mu)}(t) \rangle\rangle_{\text{ss}}}{|\alpha_\omega^\mu|^2} + \frac{\langle\langle a_{\text{out}}^{\text{loss} \dagger}(t) a_{\text{out}}^{\text{loss}}(t) \rangle\rangle_{\text{ss}}}{|\alpha_\omega^\mu|^2} = 1. \quad (\text{D.5})$$

References

- [1] Roy D, Wilson C M, and Firstenberg O 2017 Colloquium: Strongly interacting photons in one-dimensional continuum *Rev. Mod. Phys.* **89** 021001
- [2] Chang D E, Douglas J S, González-Tudela A, Hung C -L, and Kimble H J 2018 Colloquium: Quantum matter built from nanoscopic lattices of atoms and photons *Rev. Mod. Phys.* **90** 031002
- [3] Astafiev O, Zagoskin A M, Abdumalikov A A, Pashkin Y A, Yamamoto T, Inomata K, Nakamura Y and Tsai J S 2010 Resonance Fluorescence of a Single Artificial Atom *Science* **327** 840
- [4] Hoi I-C, Kockum A F, Palomaki T, Stace T M, Fan B, Tornberg L, Sathyamoorthy S R, Johansson G, Delsing P, and Wilson C M 2013 Giant Cross-Kerr Effect for Propagating Microwaves Induced by an Artificial Atom *Phys. Rev. Lett.* **111** 053601
- [5] Eder P, Ramos T, Goetz J, Fischer M, Pogorzalek S, Martínez J P, Menzel E P, Loacker F, Xie, E, García-Ripoll J J, Fedorov K G, Marx A, Deppe F, Gross R 2018 Quantum probe of an on-chip broadband interferometer for quantum microwave photonics, *Supercond. Sci. Technol.* (in press)
- [6] Gu X, Kockum A F, Miranowicz A, Liu Y, and Nori F 2017 Microwave photonics with superconducting quantum circuits *Phys. Rep.* **718-719** 1-102
- [7] Reitz D, Sayrin C, Mitsch R, Schneeweiss P, and Rauschenbeutel A 2013 Coherence Properties of Nanofiber-Trapped Cesium Atoms *Phys. Rev. Lett.* **110** 243603
- [8] Tiecke T G, Thompson J D, de Leon N P, Liu L R, Vuletić V, and Lukin M D 2014 Nanophotonic quantum phase switch with a single atom *Nature* **508** 241
- [9] Goban A, Hung C-L, Hood J D, Yu S-P, Muniz J A, Painter O, and Kimble H J 2015 Superradiance for Atoms Trapped along a Photonic Crystal Waveguide *Phys. Rev. Lett.* **115** 063601
- [10] Solano P, Barberis-Blostein P, Fatemi F K, Orozco L A, Rolston S L 2017 Super-radiance reveals infinite-range dipole interactions through a nanofiber *Nature Comm.* **8** 1857
- [11] Wrigge G, Gerhardt I, Hwang J, Zumofen G, and Sandoghdar V 2008 Efficient coupling of photons to a single molecule and the observation of its resonance fluorescence *Nature Phys.* **4** 60
- [12] Arcari M, Söllner I, Javadi A, Lindskov Hansen S, Mahmoodian S, Liu J, Thyrrestrup H, Lee E H, Song J D, Stobbe S, and Lodahl P 2014 Near-Unity Coupling Efficiency of a Quantum Emitter to a Photonic Crystal Waveguide *Phys. Rev. Lett.* **113** 093603

- [13] Yalla R, Sadgrove M, Nayak K P, Hakuta K 2014 Cavity Quantum Electrodynamics on a Nanofiber Using a Composite Photonic Crystal Cavity *Phys. Rev. Lett.* **113** 143601
- [14] Coles R J, Price D M, Dixon J E., Royall B, Clarke E, Kok P, Skolnick M S, Fox A M, and Makhonin M N 2016. Chirality of nanophotonic waveguide with embedded quantum emitter for unidirectional spin transfer *Nature Comm.* **7** 11183
- [15] Forn-Díaz P, García-Ripoll J J, Peropadre B, Orgiazzi J-L, Yurtalan M A, Belyansky R, Wilson C M, and Lupascu A 2017 Ultrastrong coupling of a single artificial atom to an electromagnetic continuum in the nonperturbative regime *Nat. Phys.* **13** 39
- [16] Magazzu L, Forn-Díaz P, Belyansky R, Orgiazzi J-L, Yurtalan M A, Otto M R, Lupascu A, Wilson C M, and Grifoni M 2018 Probing the strongly driven spin-boson model in a superconducting quantum circuit *Nat. Comm.* **9** 1403
- [17] Shen J -T, and Fan S 2005 Coherent photon transport from spontaneous emission in one-dimensional waveguides *Opt. Lett.* **30** 2001
- [18] Shen J-T, and Fan S 2007 Strongly Correlated Two-Photon Transport in a One-Dimensional Waveguide Coupled to a Two-Level System *Phys. Rev. Lett.* **98** 153003
- [19] Zheng H, Gauthier D J, and Baranger H U 2010 Waveguide QED: Many-body bound-state effects in coherent and Fock-state scattering from a two-level system *Phys. Rev. A* **82** 063816
- [20] Fan S, Kocabas S E and Shen J T 2010 Input-output formalism for few-photon transport in one-dimensional nanophotonic waveguides coupled to a qubit *Phys. Rev. A* **82** 063821
- [21] Caneva T, Manzoni M T, Shi T, Douglas J S, Cirac J I and Chang D E 2015 Quantum dynamics of propagating photons with strong interactions: a generalized input-output formalism *New J. Phys.* **17** 113001
- [22] Sánchez-Burillo E, Martín-Moreno L, Zueco D, and García-Ripoll J J 2016 One- and two-photon scattering from generalized V-type atoms *Phys. Rev. A* **94** 053857
- [23] Roulet A, and Scarani V 2016 Solving the scattering of N photons on a two-level atom without computation *New J. Phys.* **18** 093035
- [24] See T F, Noh C, and Angelakis D G 2017 Diagrammatic approach to multiphoton scattering. *Phys. Rev. A* **95** 053845
- [25] Hurst D L and Kok P 2018 Analytic few-photon scattering in waveguide QED *Phys. Rev. A* **97** 043850
- [26] Shi T, and Sun C P 2009 Lehmann-Symanzik-Zimmermann reduction approach to multiphoton scattering in coupled-resonator arrays *Phys. Rev. B* **79** 205111
- [27] Shi T, Chang D E and Cirac J I 2015 Multiphoton-scattering theory and generalized master equations *Phys. Rev. A* **92** 053834
- [28] Paladino E, Galperin Y M, Falci G, and Altshuler B L 2014 $1/f$ noise: Implications for solid-state quantum information *Rev. Mod. Phys.* **86** 361418
- [29] Ithier G, Collin E, Joyez P, Meeson P J, Vion D, Esteve D, Chiarello F, Shnirman A, Makhlin Y, Schrieffer J and Schön G 2005 Decoherence in a superconducting quantum bit circuit *Phys. Rev. B* **72** 134519
- [30] Deppe F, Mariantoni M, Menzel E P, Saito S, Kakuyanagi K, Tanaka H, Meno T, Semba K, Takayanagi H, and Gross R 2007 Phase coherent dynamics of a superconducting flux qubit with capacitive bias readout *Phys. Rev. B* **76** 214503
- [31] Meriles C A, Jiang L, Goldstein G, Hodges J S, Maze J, Lukin M D, and Cappellaro P 2010 Imaging mesoscopic nuclear spin noise with a diamond magnetometer *J. Chem. Phys.* **133** 124105
- [32] Bylander J, Gustavsson S, Yan F, Yoshihara F, Harrabi K, Fitch G, Cory D G, Nakamura Y, Tsai J S, and Oliver W D 2011 Noise spectroscopy through dynamical decoupling with a superconducting flux qubit *Nature Phys.* **7** 565
- [33] O'Malley P, Kelly J, Barends R, Campbell B, Chen Y, Chen Z, Chiaro B, Dunsworth A, Fowler A, Hoi I C, Jeffrey E, Megrant A, Mutus J, Neill C, Quintana C, Roushan P, Sank D, Vainsencher A, Wenner J, White T, Korotkov A, Cleland A and Martinis J M 2015 Qubit Metrology of Ultralow Phase Noise Using Randomized Benchmarking *Phys. Rev. Applied* **3** 044009
- [34] Roumach Y, Müller C, Unden T, Rogers L J, Isoda T, Itoh K M, Markham M, Stacey A, Meijer J,

- Pezzagna S, Naydenov B, McGuinness L P, Bar-Gill N, and Jelezko F 2015 Spectroscopy of Surface-Induced Noise Using Shallow Spins in Diamond *Phys. Rev. Lett.* **114** 017601
- [35] Éthier-Majcher G, Gangloff D, Stockill R, Clarke E, Hugues M, Le Gall C, and Atatüre M 2017 Improving a Solid-State Qubit through an Engineered Mesoscopic Environment *Phys. Rev. Lett.* **119** 130503
- [36] Norris L M, Lucarelli D, Frey V M, Mavadia S, Biercuk M J, and Viola L 2018 Optimally band-limited spectroscopy of control noise using a qubit sensor *Phys. Rev. A* **98** 032315
- [37] Álvarez G A, and Suter D 2011 Measuring the Spectrum of Colored Noise by Dynamical Decoupling *Phys. Rev. Lett.* **107** 230501
- [38] Norris L M, Paz-Silva G A, and Viola L 2016 Qubit Noise Spectroscopy for Non-Gaussian Dephasing Environments *Phys. Rev. Lett.* **116** 150503
- [39] Mavadia S, Edmunds C L, Hempel C, Ball H, Roy F, Stace T M, and Biercuk M J 2018 Experimental quantum verification in the presence of temporally correlated noise *npj Quantum Information* **4** 7
- [40] Lisenfeld J, Bilmes A, Matityahu S, Zanker S, Marthaler M, Schechter M, Schön G, Shnirman A, Weiss G, and Ustinov A V, 2016 Decoherence spectroscopy with individual two-level tunneling defects *Scientific Reports* **6** 23786
- [41] Kammerer C, Cassabois G, Voisin C, Perrin M, Delalande C, Roussignol P, and Gérard J M 2002 Interferometric correlation spectroscopy in single quantum dots *Appl. Phys. Lett.* **81** 2737
- [42] Berthelot A, Favero I, Cassabois G, Voisin C, Delalande C, Roussignol P, Ferreira R, and Gérard J M 2006 Unconventional motional narrowing in the optical spectrum of a semiconductor quantum dot *Nature Phys.* **2** 759
- [43] Coolen L, Brokmann X, Spinicelli P, Hermier J -P 2008 Emission Characterization of a Single CdSe-ZnS Nanocrystal with High Temporal and Spectral Resolution by Photon-Correlation Fourier Spectroscopy *Phys. Rev. Lett.* **100** 027403
- [44] Sallen G, Tribu A, Aichele T, André R, Besombes L, Bougerol C, Richard M, Tatarenko S, Kheng K, and Poizat J -P 2010 Subnanosecond spectral diffusion measurement using photon correlation *Nat. Photonics* **4** 696
- [45] Wolters J, Sadzak N, Schell A W, Schröder T, Benson O 2013 Measurement of the Ultrafast Spectral Diffusion of the Optical Transition of Nitrogen Vacancy Centers in Nano-Size Diamond Using Correlation Interferometry *Phys. Rev. Lett.* **110** 027401
- [46] Thoma A, Schnauber P, Gschrey M, Seifried M, Wolters J, Schulze J H, Strittmatter A, Rodt S, Carmele A, Knorr A, Heindel T and Reitzenstein S 2016 Exploring Dephasing of a Solid-State Quantum Emitter via Time- and Temperature-Dependent Hong-Ou-Mandel Experiments *Phys. Rev. Lett.* **116** 033601
- [47] Kubo R 1963 Stochastic Liouville Equations *J. Math. Phys.* **4** 174
- [48] Geva E and Skinner J L 1997 Theory of Single-Molecule Optical Line-Shape Distributions in Low-Temperature Glasses *J. Phys. Chem. B* **101** 8920
- [49] Ramos T, and García-Ripoll J J 2017 Multiphoton Scattering Tomography with Coherent States, *Phys. Rev. Lett.* **119** 153601
- [50] Jacobs K 2010 *Stochastic processes for physicists* (Cambridge University Press)
- [51] van Kampen N 1992 *Stochastic Processes in Physics and Chemistry* (Amsterdam: Elsevier)
- [52] Gardiner C W 1985 *Handbook of stochastic methods* (Springer Verlag Berlin Heidelberg)
- [53] Gardiner C W, and Collett, M J 1985 Input and output in damped quantum systems: Quantum stochastic differential equations and the master equation *Phys. Rev. A* **31** 3761
- [54] Gardiner C W, and Zoller P 2004 *Quantum Noise* (Springer-Verlag Berlin Heidelberg).
- [55] Roy D 2010 Few-photon optical diode *Phys. Rev. B* **81** 155117
- [56] Ramos T, Pichler H, Daley A J and Zoller P 2014 Quantum Spin Dimers from Chiral Dissipation in Cold-Atom Chains *Phys. Rev. Lett.* **113** 237203
- [57] Lodahl P, Mahmoodian S, Stobbe S, Rauschenbeutel A, Schneeweiss P, Volz J, Pichler H, and Zoller P 2017 Chiral quantum optics *Nature* **541** 473
- [58] Kotler S, Akerman N, Glickman Y, Ozeri R 2013 Nonlinear Single-Spin Spectrum Analyzer *Phys. Rev. Lett.* **110** 110503

- [59] Thyrrstrup H, Kirsanske G, Jeannic H L, Pregolato T, Zhai L, Raahauge L, Midolo L, Rotenberg N, Javadi A, Schott R, Wieck A D, Ludwig A, Löbl M C, Söllner I, Warburton R J, and Lodahl P 2018 Quantum Optics with Near-Lifetime-Limited Quantum-Dot Transitions in a Nanophotonic Waveguide *Nano Lett.* **18** [7b05016](#)
- [60] Javadi A, Söllner I, Arcari M, Hansen S L, Midolo L, Mahmoodian S, Kiransk G, Pregolato T, Lee E H, Song J D, Stobbe S, and Lodahl P 2015 Single-photon non-linear optics with a quantum dot in a waveguide *Nat. Comm.* **6** [8655](#)
- [61] Peropadre B, Lindkvist J, Hoi I -C, Wilson C M, Garcia-Ripoll J J, Delsing P, Johansson G 2013 Scattering of coherent states on a single artificial atom *New J. Phys.* **15** [035009](#)
- [62] Petrakis L 1967 Spectral line shapes: Gaussian and Lorentzian functions in magnetic resonance *J. Chem. Educ.* **44** [432](#)
- [63] Galperin Y M, Altshuler B L, Bergli J, and Shantsev D V 2006 Non-Gaussian Low-Frequency Noise as a Source of Qubit Decoherence *Phys. Rev. Lett.* **96** [097009](#)
- [64] Koch R H, DiVincenzo D P, and Clarke J 2007 Model for $1/f$ Flux Noise in SQUIDs and Qubits *Phys. Rev. Lett.* **98** [267003](#)
- [65] Eliazar I, and Klafter, J 2010 Universal generation of $1/f$ noises *Phys. Rev. E* **82** [021109](#)
- [66] Quintana C M, Chen Y, Sank D, Petukhov A G, White T C, Kafri D, Chiaro B, Megrant A, Barends R, Campbell B, Chen Z, Dunsworth A, Fowler A G, Graff R, Jeffrey E, Kelly J, Lucero E, Mutus J Y, Neeley M, Neill C, OMalley P J J, Roushan P, Shabani A, Smelyanskiy V N, Vainsencher A, Wenner J, Neven H, and Martinis J M 2017 Observation of Classical-Quantum Crossover of $1/f$ Flux Noise and Its Paramagnetic Temperature Dependence *Phys. Rev. Lett.* **118** [057702](#)
- [67] Pachón L A, Relaño A, Peropadre B, and Aspuru-Guzik A 2018 Origin of the $1/f^\alpha$ -Spectral-Noise in Chaotic and Regular Quantum Systems *Phys. Rev. E* [042213](#)
- [68] Paladino E, Faoro L, Falci G, and Fazio R 2002 Decoherence and $1/f$ Noise in Josephson Qubits *Phys. Rev. Lett.* **88** [228304](#)
- [69] Shnirman A, Schön G, Martin I, and Makhlin Y 2005 Low- and High-Frequency Noise from Coherent Two-Level Systems *Phys. Rev. Lett.* **94**, [127002](#)
- [70] Galperin Y M, Altshuler B L, Bergli J, Shantsev D, and Vinokur V 2007 Non-Gaussian dephasing in flux qubits due to $1/f$ noise *Phys. Rev. B* **76** [064531](#)
- [71] Ruseckas J, and Kaulakys B 2010 $1/f$ noise from nonlinear stochastic differential equations *Phys. Rev. E* **81** [031105](#)
- [72] Kaulakys B, Gontis V, and Alaburda M 2005 Point process model of $1/f$ noise vs a sum of Lorentzians *Phys. Rev. E* **71** [051105](#)
- [73] Maser A, Gmeiner B, Götzinger S, Utikal T, and Sandoghdar V 2016 Few-photon coherent nonlinear optics with a single molecule *Nature Photon.* **10** [450](#)
- [74] Sipahigil A, Evans R E, Sukachev D D, Burek M J, Borregaard J, Bhaskar M K, Nguyen C T, Pacheco J L, Atikian H A, Meuwly C, Camacho R M, Jelezko F, Bielejec E, Park H, Loncar, and M Lukin M D 2016 An integrated diamond nanophotonics platform for quantum optical networks *Science* **354** [847](#)
- [75] Fano U 1961 Effects of Configuration Interaction on Intensities and Phase Shifts *Phys. Rev.* **124** [1866](#)
- [76] Zhou L, Gong Z R, Liu Y, Sun C P, and Nori F 2008 Controllable Scattering of a Single Photon inside a One-Dimensional Resonator Waveguide *Phys. Rev. Lett.* **101** [100501](#)
- [77] Auffeves-Garnier A, Simon C, Gérard J -M, and Poizat J -P 2007 Giant optical nonlinearity induced by a single two-level system interacting with a cavity in the Purcell regime *Phys. Rev. A* **75** [053823](#)
- [78] Kocabas, S E, Rephaeli E, and Fan S 2012 Resonance fluorescence in a waveguide geometry *Phys. Rev. A* **85** [023817](#)
- [79] Lemonde M -A, Meesala S, Sipahigil A, Schuetz M J A, Lukin M D, Loncar M, and Rabl P 2018 Phonon Networks with Silicon-Vacancy Centers in Diamond Waveguides *Phys. Rev. Lett.* **120** [213603](#)
- [80] Martín-Cano D, Huidobro P A, Moreno E, and García-Vidal F J 2014 Quantum Plasmonics *Handbook of Surface Science* **4** [349](#) (Amsterdam: Elsevier)
- [81] Araneda G, Higginbottom D B, Slodicka L, Colombe Y, and Blatt R 2018 Interference of Single Photons

- Emitted by Entangled Atoms in Free Space *Phys. Rev. Lett.* **120** 193603
- [82] Suter D, and Álvarez G A 2016 Colloquium: Protecting quantum information against environmental noise *Rev. Mod. Phys.* **88** 041001
- [83] Németh N, Parkins S, Knorr A, and Carmele A 2018 Stabilizing quantum coherence against pure dephasing in the presence of quantum feedback at finite temperature, [arXiv:1805.02317](https://arxiv.org/abs/1805.02317)
- [84] Paz-Silva G A, Norris L M, and Viola L 2017 Multiqubit spectroscopy of Gaussian quantum noise *Phys. Rev. A* **95** 022121
- [85] Szańkowski P, Trippenbach M, and Cywiński L 2016 Spectroscopy of cross correlations of environmental noises with two qubits *Phys. Rev. A* **94** 012109
- [86] Prasanna Venkatesh B, Juan M L, and Romero-Isart O 2018 Cooperative Effects in Closely Packed Quantum Emitters with Collective Dephasing *Phys. Rev. Lett.* **120** 033602
- [87] Phillips W A 1987 Two-level states in glasses *Rep. Prog. Phys.* **50** 1657
- [88] Ramos T, Sudhir V, Stannigel K, Zoller P, and Kippenberg T J 2013 Nonlinear Quantum Optomechanics via Individual Intrinsic Two-Level Defects *Phys. Rev. Lett.* **110** 193602
- [89] Simmonds R W, Lang K M, Hite D A, Nam S, Pappas D P, and Martinis J M 2004 Decoherence in Josephson Phase Qubits from Junction Resonators *Phys. Rev. Lett.* **93** 077003
- [90] Astafiev O, Pashkin Y A, Nakamura Y, Yamamoto T, and Tsai J S 2004 Quantum Noise in the Josephson Charge Qubit *Phys. Rev. Lett.* **93** 267007
- [91] Hu Y, Cai Z, Baranov M A and Zoller P 2015 Majorana fermions in noisy Kitaev wires *Phys. Rev. B* **92** 165118
- [92] Shen J -T. and Fan S 2009 Theory of single-photon transport in a single-mode waveguide. I. Coupling to a cavity containing a two-level atom *Phys. Rev. A* **79**023837